Biol. Cell (2021) **113,** 344–373 DOI: 10.1111/boc.202000110

Review

Dynamic interplay between cell membrane tension and clathrin-mediated endocytosis

Umidahan Djakbarova*, Yasaman Madraki*, Emily T. Chan†‡ and Cömert Kural*†[1]

*Department of Physics, The Ohio State University, Columbus, OH 43210, USA, †Interdisciplinary Biophysics Graduate Program, The Ohio State University, Columbus, OH 43210, USA, and ‡Molecular Biophysics Training Program, The Ohio State University, Columbus, OH 43210, USA

Deformability of the plasma membrane, the outermost surface of metazoan cells, allows cells to be dynamic, mobile and flexible. Factors that affect this deformability, such as tension on the membrane, can regulate a myriad of cellular functions, including membrane resealing, cell motility, polarisation, shape maintenance, membrane area control and endocytic vesicle trafficking. This review focuses on mechanoregulation of clathrin-mediated endocytosis (CME). We first delineate the origins of cell membrane tension and the factors that yield to its spatial and temporal fluctuations within cells. We then review the recent literature demonstrating that tension on the membrane is a fast-acting and reversible regulator of CME. Finally, we discuss tension-based regulation of endocytic clathrin coat formation during physiological processes.

Introduction

Ordered transport of lipids and proteins between membrane-bound organelles is essential for maintaining the organisation and function of cells. Endocytosis accounts for an important part of this traffic by facilitating internalisation of plasma membrane patches and proteins in the form of vesicles [Conner and Schmid, 2003]. Clathrin-coated membrane carriers are responsible for a major fraction of endocytic traffic between the plasma membrane and endosomes [Kirchhausen, 1993]. The loss of function of the central components of clathrin-mediated endocytosis (CME) results in embryonic lethality [Chen et al., 2009, Ferguson et al., 2009, Mitsunari et al., 2005] and its perturbation is linked to numerous human disorders, such as cancer, myopathies, psychiatric and neurodegenerative disorders including Alzheimer's disease [Bitoun et al., 2005, Dalgliesh et al., 2010, Harold et al., 2009, Kan et al., 2010, McMahon and Boucrot, 2011, Mishra et al., 2002, Treusch et al., 2011, Wettey, 2002]. CME involves assembly of clathrin into a multifaceted coat (80–200 nm in diameter) on the inner leaflet of the plasma membrane, which leads to formation of small invaginations called clathrin-coated pits [Edeling et al., 2006; Robinson, 2004] (Figures 1A and 1B). This growth is mediated by an orchestrated recruitment of coat proteins to the plasma membrane. Spatiotemporal coordination of these proteins provides the energy necessary for extensive membrane remodelling and, subsequently, membrane invagination deepens with the growing

[1]To whom correspondence should be addressed (e-mail: kural.1@osu.edu)

Key words: Cellular imaging, Cell migration/adhesion, Clathrin, Endocytosis/exocytosis, Membrane trafficking, Membrane tension.

Abbreviations: AFM, atomic force microscopy; ANTH, AP180 N-terminal homology; AP2, adaptor protein 2; Arp2/3, actin-related protein-2/3; AS, amnioserosa; BAR, Bin1-Amphiphysin-Rvs; CALM, clathrin assembly lymphoid myeloid leukemia; CD4, cluster of differentiation 4; CLIC/GEEC, clathrin-independent carriers/glycosylphosphotidylinositol-anchored protein-enriched compartments; CME, clathrin-mediated endocytosis; EGF, epidermal growth factor; EGFR, epidermal growth factor receptor; EM, electron microscopy; ENTH, epsin N-terminal homology; Eps15, epidermal growth factor receptor substrate 15; FBP17, formin binding protein 17; FCHo1/2, F-BAR domain-containing Fer/Cip4 homology domain-only proteins 1 and 2; FliptR, fluorescent lipid tension reporter; F-MMM, fluid mosaic membrane model; G1, phase growth phase 1; G2, phase growth phase 2; GFP, green fluorescent protein; Hsc70, heat shock cognate 70; LDL, low-density lipoproteins; LE, lateral epidermis; PDMS, polydimethylsiloxane; PICALM, phosphatidylinositol-binding clathrin assembly protein; PtdIns(4,5)P2, phosphatidylinositol 4,5-bisphosphate; ROI, region of interest; S phase, synthesis phase; SD, standard deviation; SIM, structured illumination microscopy; STORM, stochastic optical reconstruction microscopy; TCAL, tubular clathrin/AP-2 lattice structures; TIRF, total internal reflection fluorescence; TIRF-SIM, total internal reflection fluorescence structured illumination microscopy; WASP, Wiskott Aldrich Syndrome Protein; WAVE, WASP-family verprolin- homologous protein

Figure 1 | See Legend on next page

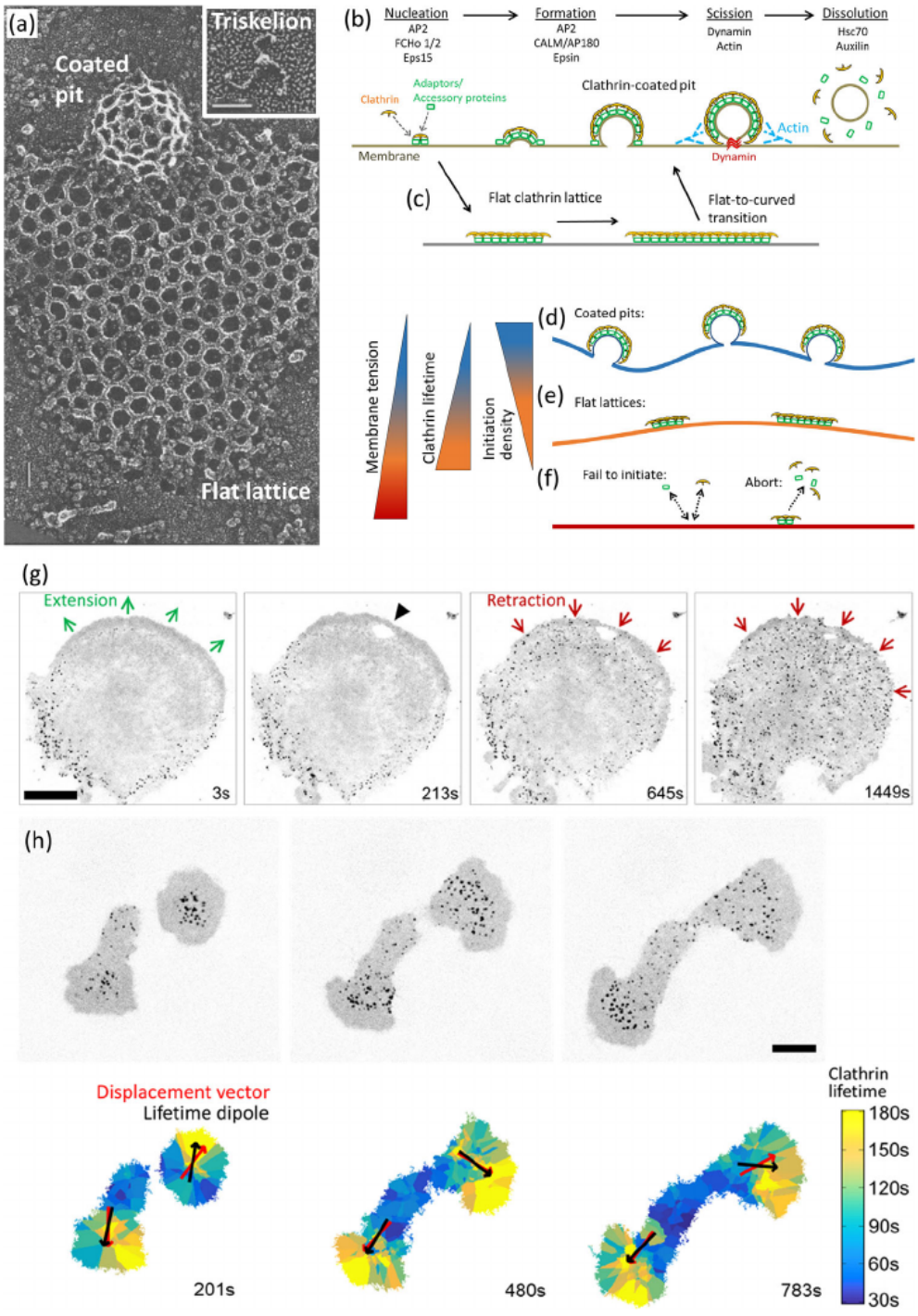

pit until it is pinched off, generating a clathrin-coated vesicle. After separating from the membrane, the newly formed vesicle rapidly diffuses within the cytoplasm while shedding its coat of clathrin and adaptor proteins through the uncoating reaction (Figure 1B).

Clathrin-coated structures have been the most extensively studied intracellular membrane

Figure 1 | Structural and dynamic heterogeneity of endocytic clathrin-coated structures

(**a**) Quick-freeze deep-etch electron microscopy images show coats of distinct geometries that clathrin triskelions (inset) can assemble into, that is, highly curved pits and flat lattices. Scale bars, 33 nm. Reproduced, with permission, from Heuser et al. (1987). (**b**) Initiation (nucleation), formation (growth), scission (budding) and dissolution (uncoating) phases of endocytic clathrin vesicle formation are depicted according to the constant curvature model [Kirchhausen, 2009, Willy et al., 2019]. In this model, curvature is initiated and maintained by adaptor-mediated recruitment of clathrin triskelions to the plasma membrane. Various adaptor/accessory proteins take action at different stages. (**c**) An alternative (flat-to-curved transition) model predicts that flat clathrin arrays are the precursors of curved clathrin pits: the bending of the membrane takes place rather abruptly after the coat area reaches a critical threshold [Avinoam et al., 2015, Sochacki and Taraska, 2019]. (**d**) The energy cost of membrane bending is at the minimum when the tension is low. This allows formation of curved and dynamic clathrin pits. (**e**) Clathrin arrays with lower curvature levels are formed on surfaces with moderate tension [Saleem et al., 2015]. These structures have slower internalisation dynamics (i.e., longer lifetimes) compared with clathrin pits [Ferguson et al., 2016, Saffarian et al., 2009, Batchelder and Yarar, 2010]. (**f**) Increased membrane tension can lead to complete inhibition of clathrin coat formation [Saleem et al., 2015] either due to hindered initiation or premature disassembly (abortion). (**g**) Fluorescence images (inverted) show clathrin coats at the ventral surface of a cultured cell originally extending toward the top-right corner of the field of view. Each spot corresponds to an individual endocytic clathrin coat. The lamella ceases to extend and begins to retract upon contact with a micromanipulator-controlled glass tip (the site of contact is marked by the black arrowhead). Retraction of the lamella is accompanied by a rapid increase in the initiation rate of endocytic clathrin coats at the ventral surface. Scale bar, 20 μm. Reproduced, with permission, from Ferguson et al. (2017). (**h**) Fluorescence images (inverted) show clathrin coats at the ventral surface of two asymmetrically spreading cells (upper panel). Clathrin coat lifetime maps assembled for the same cells demonstrate the spatial heterogeneity in CME dynamics at various stages of spreading (lower panel). Significant correlation between the lifetime dipoles (vector pointing toward the area with longer clathrin coat lifetimes) and displacement of cells affirm the front-to-rear tension gradient in migrating cells. Scale bar, 10 μm. Reproduced, with permission, from Willy et al. (2017).

transporters since their discovery in 1975 [Pearse, 1975, Robinson, 2015, Schmid, 1997]. A multitude of biophysical and biochemical methodologies have been employed to elucidate the structural and dynamic properties of endocytic clathrin coats [Robinson, 2015]. Structural characterisation goes back to electron microscopy (EM) studies conducted more than four decades ago [Heuser, 1980, Kanaseki and Kadota, 1969, Pearse, 1975]. Biochemical assays led to the discovery that the basic unit of the clathrin coat is a heterohexameric complex, termed as a clathrin triskelion, that is composed of three copies of clathrin heavy chain and three light chains (Figure 1A) [Kirchhausen and Harrison, 1981]. While clathrin heavy chains are essential structural components of the coats, the light chains have more regulatory functions [Biancospino et al., 2019, Tsygankova and Keen, 2019, Wilbur et al., 2010, Wu et al., 2016, Ybe, 1998]. During formation of endocytic vesicles, clathrin triskelions polymerise into hexagonal and pentagonal faces. Purely hexagonal faces give rise to flat lattices, whereas the incorporation of pentagons promotes curvature formation [Heuser et al., 1987] (Figure 1A), where 12 pentagons are required for closure of the pit into a coated vesicle [Musacchio et al., 1999, Shraiman, 1997]. Although clathrin triskelions form the tessellated polygonal scaffold that is the mechanical backbone of clathrin coats, they cannot directly bind to membrane components. Interaction of clathrin with the plasma membrane is mediated by a mosaic of adaptor proteins (primarily AP2; Figure 1B) [Sochacki et al., 2017, Taylor et al., 2011, Unanue et al., 1981], some of which are directly involved in curvature generation.

Several modes of clathrin coat assembly and membrane curvature generation were proposed based on electron micrographs of endocytic clathrin coats at different stages of assembly [Harrison and Kirchhausen, 1983, Heuser et al., 1987, Mashl and Bruinsma, 1998] (Figures 1A–1C). Characterisation of the structural features of clathrin-coats via EM and X-ray crystallography [Heuser, 1980, Musacchio et al., 1999, Smith, 1998] is followed by applications of advanced fluorescence imaging aimed for monitoring CME dynamics within living cells [Ehrlich et al., 2004, Kural and Kirchhausen, 2012, Kural et al., 2012, Kural et al., 2015, Mettlen and Danuser, 2014]. Seminal studies conducted at the beginning of the last decade demonstrated that cell mechanics,

changes in plasma membrane tension in particular, can give rise to dynamically distinct populations of clathrin-coated structures within cells (Figures 1D–1F) [Aghamohammadzadeh and Ayscough, 2009, Boulant et al., 2011]. Following research revealed that spatiotemporal variations in plasma membrane tension is the principal factor behind the heterogeneity in CME within cells and tissues (Figures 1G and 1H) [Ferguson et al., 2016, Ferguson et al., 2017, Kaur et al., 2014, Tan et al., 2015, Willy et al., 2017]. In the first section of this review, we discuss the latest findings on propagation and spatial distribution of tension on the cell membrane along with the state-of-the-art approaches developed to quantify tension gradients within live cells. We then focus on tension-mediated regulation of endocytic clathrin coat formation in living cells. In doing so, we introduce cutting-edge imaging tools that enable quantitative analyses of endocytosis dynamics within cells and multicellular organisms. Finally, we expound on the recent literature unraveling how spatial and temporal fluctuations in membrane tension result in heterogeneous CME activity during central physiological processes.

Physics of the plasma membrane

Plasma membrane is the interface between a cell and its environment. It holds the cellular contents (i.e., cytoplasm) together, regulates exchange of molecules with the extracellular milieu, and defines the cell shape. When a membrane-bound system is in a state of equilibrium, the difference between the internal and external pressures is expected to be balanced by a uniform tension throughout the membrane. However, a living cell is out of equilibrium. The changes in intra- and extra-cellular pressures, production and consumption of energy through biochemical reactions, generation of forces by cytoskeletal motors and filaments, and heterogeneity in membrane composition result in spatiotemporal variations in local membrane curvature, rigidity and tension.

A growing body of research has demonstrated regulatory roles of membrane tension on central processes, including membrane trafficking, the cell cycle, differentiation, signalling, migration and mechanosensation [Apodaca, 2002, Batchelder et al., 2011, Fogelson and Mogilner, 2014, Gauthier et al., 2009, Gauthier et al., 2011, Houk et al., 2012, Keren, 2011, Keren et al., 2008, Lieber et al., 2015, Raucher and Sheetz, 2000, Sheetz, 2001, Sheetz and Dai, 1996, Sheetz et al., 2006]. Therefore, it is important to understand how tension is originated on the membrane, and how it is distributed and propagated throughout the cell when a perturbation occurs.

The origins of the plasma membrane tension

Lipid molecules form a thin film around the cytoplasm as a manifestation of surface tension on the cell membrane. In eukaryotic cells, the apparent membrane tension has two major contributors: in-plane tension required to overcome the hydrostatic pressure within the cell and the adhesive interaction between the cell membrane and the underlying cytoskeleton [Dai and Sheetz, 1995, Waugh and Bauserman, 1995]. The apparent membrane tension measured by experimental techniques is a combination of both in-plane tension and the membrane–cytoskeleton adhesion.

Membrane–cytoskeleton adhesion is associated with the linkage of the phospholipid-binding proteins with the actin cortex, and therefore is dependent on local polymerisation and/or contraction of actin filaments [Gauthier et al., 2012] (Figure 2A). Thus, membrane–cytoskeleton adhesion is dynamic and non-homogeneous throughout the cell membrane. When it weakens locally or gaps appear on the cytoskeletal cortex, hydrostatic pressure gives rise to blebs on the cell membrane [Dai and Sheetz, 1999] (Figure 2B). The absence of actin filaments within blebs shows that blebbing regions of the plasma membrane are detached from the actin cortex [Cunningham, 1995]. Consequently, the main contribution to tension measured in blebs is the in-plane tension, which is a uniform molecular attraction within the membrane [Dai and Sheetz, 1999]. However, measurements in the parts of membrane attached to the cytoskeleton show a non-uniform spatial tension distribution [Dai and Sheetz, 1999, Shi et al., 2018]. Additional evidence shows that the tension perturbation diffuses very quickly within blebs, unlike the regions of the plasma membrane attached to the cytoskeleton [Shi et al., 2018]. This leads us to a discussion regarding propagation of tension along the plasma membrane.

Figure 2 | Origins and quantification of membrane tension in live cells

(**a**) Schematic representations of the plasma membrane, where the phospholipid bilayer is shown in gray, proteins attached to the underlying actin cytoskeleton (green) are in red and proteins with no interaction with the cytoskeleton are in blue. (**b**) Membrane blebs form when the lipid bilayer is detached from the cytoskeleton. (**c**) The plasma membrane is modelled as a viscous fluid flowing through immobile proteins with the Darcy permeability (*k*) used to obtain the diffusion coefficient. (**d**) Micropipette aspiration allows the use of Laplace's law for determining the tension as a function of the membrane curvature and pressure difference between the inside and outside of the micropipette. (**e**) Membrane tether forces (*f*) measured by various force spectroscopy techniques, such as optical tweezers, can be used to quantify the tension on the membrane. (**F**) A membrane tether is generated on the surface of a fibroblast by pulling an optically trapped bead attached to the plasma membrane. Reproduced, with permission, from Gauthier et al. (2009). (**g**) Membrane tether forces measured at different stages of cell spreading demonstrate a significant reduction in membrane tension. Reproduced, with permission, from Gauthier et al. (2009). (**h**) A front-to-rear gradient in membrane tension is assessed using optical tweezers in migrating cells. Reproduced, with permission, from Lieber et al. (2015).

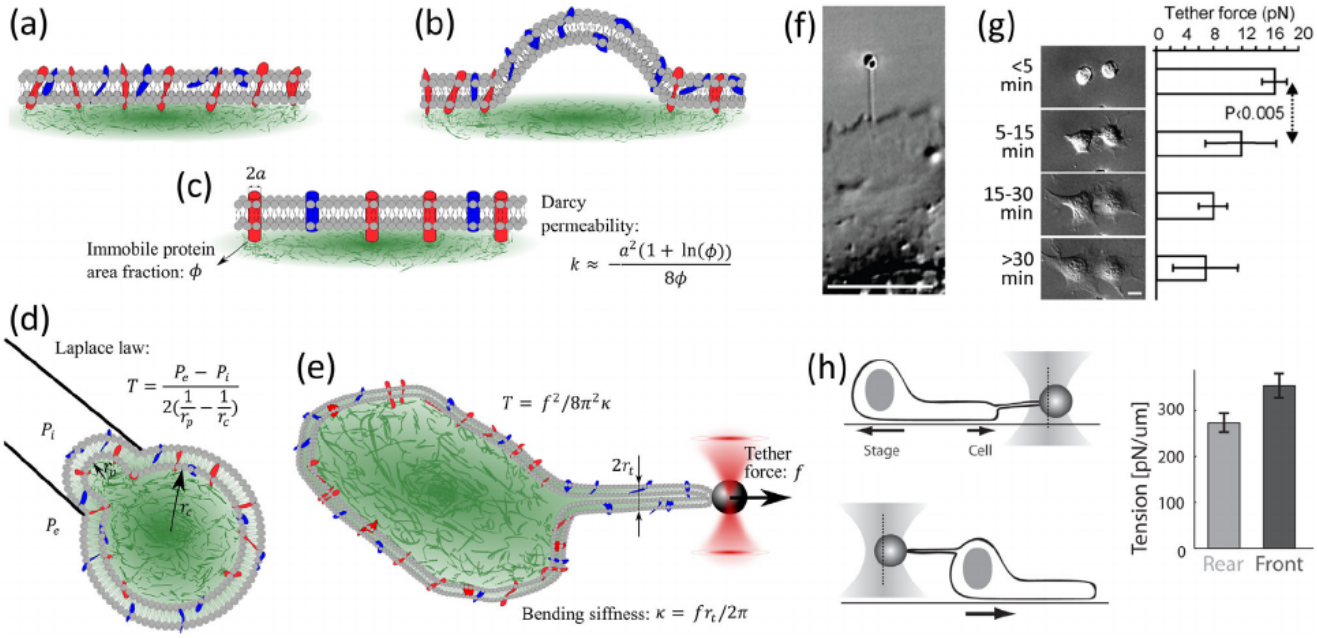

Cell membrane composition and propagation of tension

Tension propagation in a thin film is highly dependent on the mechanical characteristics of the thin film. If a tension gradient is imposed on a thin film of a viscous fluid, the fluid freely flows within the thin film and the tension propagates globally with a time scale proportional to the viscosity [Macosko, 1994]. On the other hand, tension propagation in a thin film of a semi-solid material, for example, gels, results in short-ranged diffusion and local deformation. Experiments done on the cell membrane indicate that the mechanical characteristics of the plasma membrane dictate a non-uniform tension distribution and short-range tension propagation [Shi et al., 2018]. This implies a non-linear and non-Newtonian rheological response of the plasma membrane to a tension gradient, which stems from the membrane composition and its interaction with the cytoskeleton [Larson, 1999].

The plasma membrane is composed of phosphatidylcholines, phosphatidylserines, phosphatidylethanolamines, sphingolipids, phosphoinositides and cholesterol [Keren, 2011]. The early models of the plasma membrane comprise a lipid bilayer with an asymmetric distribution of the phospholipids in the inner and outer membrane leaflets [Bretscher, 1973]. In this model, major proteins and glycoproteins were placed in their specific orientation across the membrane, and other proteins were associated

with the inner surface of the bilayer [Bretscher, 1973]. This picture was accompanied by other models which assumed that the positions of membrane lipids and proteins are stationary [Benson, 1966, Danielli and Davson, 1935, Gorter and Grendel, 1924, Stoeckenius and Engelman, 1969]. With the discovery of lipid movements within the membrane, that is, 'fluidity' [Chapman, 1975], Singer and Nicolson (1972) proposed the well-known Fluid Mosaic Membrane Model (F-MMM). The F-MMM described the membrane as a matrix of bi-layer phospholipids with inserted mobile, globular integral membrane proteins and glycoproteins. In this model, the matrix components were free to flow within the membrane plane. A few years later, experimental results reported a strong enhancement in membrane diffusion within blebs compared to the regions of the membrane intact with the cytoskeleton. This diffusion enhancement was attributed to removal of the proteins that link the plasma membrane to the cytoskeleton [Tank et al., 1982]. This indicated that not all membrane components are free to flow and that the F-MMM model needed to be modified with consideration of the complexity of membrane composition and structure. Although the lipid bilayer structure is the major component of the plasma membrane [Edidin, 2003], constraints to the flow of lipids due to interactions with the cytoskeleton and extracellular matrix have been gradually incorporated to the original model [Jacobson et al., 2019, Kusumi et al., 2012, Nicolson, 2014, Sezgin et al., 2017].

While the diffusion of transmembrane proteins within the membrane as a 2D fluid was once theoretically known to be impossible, Saffman and Delbruck described this problem by taking into account the finite viscosity of intracellular and extracellular fluids as well as the viscosity of lipid bilayer [Saffman and Delbruck, 1975]. This effort made it possible to calculate the diffusion coefficients of transmembrane proteins within the membrane. F-MMM model predicts a fluid-like behaviour, where membrane flows with a velocity $v = \Delta T/\eta$ upon generation of a tension gradient, ΔT, on the plasma membrane. Here, η is the viscosity of the lipid bilayer. Recent modifications to the F-MMM model predict that many transmembrane proteins are attached to the cytoskeleton, and therefore are the immobile components of the plasma membrane (Figures 2A–2C). These immobile components are considered to be constraints for the flow of lipids. In other words, the membrane lipid bilayer is a film of fluid flowing through a porous array of constraints [Cohen and Shi, 2020] (Figure 2C). In this framework, a tension gradient on the plasma membrane, ΔT, gives rise to a membrane flow with velocity $v = \frac{k}{\eta}\Delta T$ [Happel, 1959]. Here, k is the Darcy permeability which, in two dimensions, can be approximated for the flow of fluid through an array of stationary parallel cylinders by $k \approx -\frac{a^2(1+\ln(\phi))}{8\phi}$ (for $\phi < 0.2$) [Happel, 1959], where a is the radius of the constraint cylinders and ϕ is the in-plane area fraction that the constraints occupy within the two-dimensional membrane area (Figure 2C). This approximation indicates the drastic dependence of the Darcy permeability, hence the diffusion velocity and timescale, on the area fraction of the immobile components.

The plasma membrane is also evidenced to stretch when tugged and present resistance to flow. In this case, the tension gradient changes the area (A) according to $\Delta T = K_A \frac{\Delta A}{A}$, where K_A is the stretch modulus of the membrane. This constitutive law for the stretch in the plasma membrane is a non-linear relation, as the stretch modulus itself depends on the magnitude of the tension gradient and the initial state of the membrane. The stretch modulus can span a wide range of magnitudes (from $K_A \approx 0$ in membrane folds to $K_A \approx 100$ mN m^{-1} in pure lipid bilayer) [Evans and Rawicz, 1990, Rawicz et al., 2000]. When the plasma membrane is stretched, the lipid bilayer gradually flows over the immobile constraints to release the stretch. The diffusion coefficient in this case will be modified by the stretch modulus, $D = \frac{K_A k}{\eta}$. This modified diffusion coefficient includes both the Darcy permeability and stretch modulus. In this framework, the tension does not propagate in the membrane reservoirs and folds ($K_A \approx 0$), but it propagates very fast in blebs where the immobile constraint area fraction is negligible and the membrane is stretched. Therefore, the non-uniform composition and the complex structure of the membrane results in a spatial variation in the diffusion coefficient along the membrane and consequently, a non-uniform and localised tension distribution.

Measuring plasma membrane tension

Theoretical studies on the physical response of membranes [Agrawal and Steigmann, 2009, Edidin,

2003] and the development of force spectroscopy tools that allow membrane tension measurements in live cells [Diz-Muñoz et al., 2013] constructed the current understanding of cell membrane dynamics and their role in cellular functions. Conventional tension measurement approaches, that is, micropipette aspiration and tether pulling, are based on external micromanipulation of the membrane and measurement of the mechanical properties of the membrane as a thin film [Pontes et al., 2017]. Due to their invasive nature, these techniques are limited to isolated cells. Here, we review these traditional methods along with more recent approaches that are designed to extend the applicability of tension measurement to physiologically relevant contexts.

The micropipette aspiration technique utilises a glass pipette tip with a known diameter to apply suction on the cell membrane with a known pressure (Figure 2D) [Hochmuth, 2000]. Due to the suction pressure, a part of the cell is deformed into a hemisphere within the micropipette. The tension can be calculated using Laplace's law, $T = \frac{P_e - P_i}{2(\frac{1}{r_p} - \frac{1}{r_c})}$, based on the pressure difference between the inside and outside of the hemispherical film (P_i and P_e), and geometrical characterisation of the curvature ($\frac{1}{r_p}$ and $\frac{1}{r_c}$). While the micropipette diameter is known and the inside curvature may be estimated as hemispherical, the curvature of the cell (outside the micropipette) often cannot be estimated straightforwardly. This issue is less pronounced in suspended cells but is a limitation for cells with complex morphologies. Micropipette aspiration measures the tension in the curved part of the cell membrane, including the phospholipid bilayer and the attached cytoskeleton. Therefore, the output is a combination of membrane tension and membrane–cytoskeleton adhesion. Recent applications of this technique utilise microfluidics-based cell aspiration chambers designed to increase accuracy and throughput [Lee and Liu, 2015].

Membrane tether force measurements conducted via optical tweezers or atomic force microscopy (AFM) include attaching an adhesive surface (dielectric bead or AFM tip, respectively) to the cell membrane and pulling it away to form a thin tube of membrane, that is, membrane tether (Figures 2E and 2F). In this method, the tension is calculated using the relation $T = f^2/8\pi^2\kappa$ [Dai and Sheetz, 1999], where f is the restoring tether force applied by the tether and κ is the bending stiffness of the membrane. The bending stiffness could be found by $\kappa = fr_t/2\pi$ by measuring the tether force and the radius, r_t [Hochmuth et al., 1996, Lieber et al., 2013]. This measured force originates from tension at a specific region of the membrane from which the tether is pulled [Dai and Sheetz, 1999, Raucher and Sheetz, 2000, Sun et al., 2005, Batchelder et al., 2011, Lafaurie-Janvore et al., 2013, Lieber et al., 2013, Gabella et al., 2014, Peukes and Betz, 2014, Shi et al., 2018]. Therefore, determining the tension distribution and its propagation within the membrane necessitates multiple measurements at different regions of the membrane [Lieber et al., 2015] (Figure 2H).

Fluorescent LIPid Tension Reporter (FliptR) has been recently used as an imaging-based membrane tension reporter [Colom et al., 2018]. FliptR is fluorescent only after it is incorporated into the plasma membrane and reports the density of lipid packing through changes in fluorescence lifetime (within the range of 4–6 ns). Fluorescence lifetime imaging microscopy measurements have shown that FliptR lifetimes reduce linearly with increasing tension on the membrane. The limitation of this method stems from its nature of sensing lipid packing, which depends on both tension and lipid composition. Although tension can be calibrated uniquely for assorted lipid compositions, the variations in membrane composition cannot be detected during the measurements.

Membrane tension homeostasis

As outlined by the theoretical work of Helfrich (1973) and Canham (1970), curvature formation on a membrane requires overcoming bending energy and tension energy. The bending energy is dependent on membrane curvature and a bending modulus (in the range of 5–50 k_BT for cellular membranes [Seifert, 1997]), which is a material property of the membrane and dependent on molecular composition. Unlike the bending energy, the tension energy depends on membrane tension which is a complex variable altering along the membrane.

Membrane tension in mammalian cells is measured to be in the range of $0.001 - 3$ mN/m [Morris and Homann, 2001, Sens and Plastino, 2015]. To operate within this range and maintain tension homeostasis, mammalian cells adopt a large membrane area, which leads to membrane fluctuations and formation of membrane reservoirs such as membrane folds,

membrane wrinkles, caveolae, vacuole-like dilations and blebs under low levels of tension [Gauthier et al., 2012]. Membrane fluctuations in live cells are driven by both thermal agitation, and active, nonequilibrium forces [Turlier and Betz, 2019]. Although the physiological roles of these active fluctuations are still under investigation, we know that they exist due to evidence that the bending stiffness of membrane is on the order of thermal energy, k_BT, and that membrane tension is involved in active nonequilibrium processes. This correlation between membrane fluctuations and membrane mechanics has been used to develop a new method to determine membrane tension and bending stiffness by measuring the amplitude of the fluctuations (fluctuation spectroscopy) using weak optical tweezers [Gögler et al., 2007, Betz et al., 2009, Betz and Sykes, 2012].

Membrane reservoirs, with different shapes and sizes, play a buffering role in the variation of membrane tension. Cell membrane rapidly responds to increasing levels of tension through unfolding of membrane reservoirs [Gauthier et al., 2011, Sinha et al., 2011]. Once the reservoirs are flattened, further increases in tension are buffered by membrane trafficking pathways [Apodaca, 2002, Gauthier et al., 2012]. Endocytosis and exocytosis are opposing membrane trafficking mechanisms utilised by the cell to maintain plasma membrane turnover. High levels of membrane tension activate exocytosis, during which intracellular membrane vesicles fuse with the plasma membrane. Subsequently, membrane tension decreases due to reducing cell volume and increasing surface area [Gauthier et al., 2009, Staykova et al., 2011]. In contrast, low levels of membrane tension stimulate endocytic pathways, in which patches of the membrane are invaginated and internalised from the plasma membrane in the form of vesicles [Pinot et al., 2014, Shi and Baumgart, 2015, Loh et al., 2019]. This process increases membrane tension by increasing the cell volume and reducing the surface area [Dai et al., 1997, Raucher and Sheetz, 1999].

Local membrane tension is dynamically dictated by membrane composition and structure, forces imposed by the cytoskeleton and pressure gradients across the cell. While high levels of tension inhibit membrane deformation, low levels of local tension allow generation of membrane curvature [Shi and Baumgart, 2015]. Cells employ different mechanisms to deform the plasma membrane against tension to perform various biological functions such as endocytosis.

Generation of membrane curvature

Mechanisms of membrane curvature generation work at different scales and can be utilised simultaneously as cells undergo complex morphological changes [Keren, 2011]. At nanometer scales, curvature might be imposed by local membrane composition. Lipid molecules may have cylindrical or conical shapes depending on the size of their head group and the composition of their acyl chains. The accumulation of the lipids with conical, inverted conical and cylindrical shapes form positive, negative or zero curvatures, respectively [McMahon and Boucrot, 2015].

During formation of endocytic vesicles, a shallow membrane invagination transforms into a dome-like (hemispherical or U shaped) pit, which further leads to a closed (Ω-shaped) bud and eventually a spheroid vesicle (Figure 1B) [McMahon and Boucrot, 2011, Haucke and Kozlov, 2018]. In each step, membrane-bound proteins contribute to curvature generation in different ways. One such mechanism is insertion of amphipathic helices between phospholipids [McMahon and Gallop, 2005]. During formation of endocytic clathrin-coated vesicles, epsin and CALM adaptor proteins are recruited to PtdIns(4,5)P2-enriched membrane domains and mediate transformation of shallow invaginations into isotropically curved domes (Figure 1B) [Haucke and Kozlov, 2018]. It was proposed that membrane insertion of epsin N-terminal homology (ENTH) domain of the epsin family proteins alone is sufficient to drive the invagination of endocytic clathrin-coated structures [Ford et al., 2002]. This perception was challenged in subsequent reports as endogenous epsin concentration in a cell is inadequate to drive membrane curvature [Kirchhausen, 2012]. Indeed, proteomic studies have revealed that the relative stoichiometry of epsin is very low within endocytic coat complexes [Borner et al., 2012]. It was recently shown that epsin stabilises the curvature of clathrin-coated structures, which becomes essential for initiation and maturation of the coat under high membrane tension environments [Joseph et al., 2020]. A similar curvature generation mechanism was proposed for the amphipathic helix in the AP180 N-terminal homology (ANTH) domain of the CALM/PICALM adaptor [Miller et al., 2015]. Unlike epsin, the

stoichiometric ratio of CALM in a clathrin coat is one of the highest within the adaptor mosaic [Borner et al., 2012, Miller et al., 2015]. Indeed, as a sensor and driver of membrane curvature, CALM levels regulate the size and maturation of endocytic clathrin coats [Meyerholz et al., 2005, Miller et al., 2015]. Recent studies have revealed that the spatial distribution of PtdIns(4,5)P2 is regulated by membrane tension, where low tension triggers PtdIns(4,5)P2 clustering [Riggi et al., 2018, Riggi et al., 2019], perhaps marking a nucleation site for endocytic protein recruitment. Such a mechanism would ensure selection of the least energy costly regions of the membrane with a favourable mechanical state for endocytic vesicle formation.

Curvature can also be generated via scaffolding of the membrane by curved protein complexes [Sweitzer and Hinshaw, 1998, Peter, 2004]. For instance, BAR-domain (Bin1/amphiphysin/Rvs) proteins are characterised by elongated positively charged surfaces that interact with negatively charged membrane lipids [Simunovic et al., 2015] and oligomerise into helical bundles to generate membrane curvature [McMahon and Boucrot, 2015]. The geometry of these bundles and their interaction with the membrane are impacted by surface tension [Simunovic et al., 2015]. Each BAR protein has a different size, intrinsic curvature and membrane binding affinity, and thus are involved in distinct stages of curvature generation [Stanishneva-Konovalova et al., 2016]. FCHo 1 and 2 are F-BAR proteins that arrive at the formation sites of endocytic clathrin coats earlier than the majority of the other coat components [Taylor et al., 2011]. Therefore, it was suggested that these proteins induce the membrane curvature required for nucleation of endocytic coat assembly [Henne et al., 2010]. Furthermore, N-BAR proteins including endophilin and amphiphysin, as well as distantly related dynamin [Taylor et al., 2011], appear at later stages of endocytic vesicle formation, and are responsible for Ω-shaped bud formation and membrane fission, respectively (Figure 1B) [McMahon and Boucrot, 2011, Haucke and Kozlov, 2018, Joseph and Liu, 2020].

Coat proteins with intrinsic curvature also contribute to the underlying membrane without direct association with it [Stagg et al., 2006, Stachowiak et al., 2013]. The molecular architecture of clathrin triskelia allows adapting to different levels of curvature [Kirchhausen, 2000] and spontaneous self-assembly into clathrin cages [Ungewickell and Branton, 1981]. Clathrin triskelia recruited to liposomes by epsin adaptor proteins lacking the ENTH domain result in formation of membrane invaginations or buds [Dannhauser and Ungewickell, 2012]. Other endocytic coat proteins such as caveolin, cavin and flotinin oligomerise into scaffolds as well as insert into the membrane to mediate formation and stabilisation of curvature at caveolae [Monier et al., 1995, Frick et al., 2007, Hansen et al., 2009, Parton and Del Pozo, 2013, Parton et al., 2020]. Caveolar oligomerisation and thus curvature formation is inhibited upon acute mechanical stress which elevates membrane tension [Sinha et al., 2011]. Due to fact that caveolae have a tension-coupled curvature generation mechanism (they flatten at high tension and invaginate at low tension), they are utilised as a tension-buffering system by cells [Echarri and Del Pozo, 2015, Parton et al., 2020].

Curvature during endocytic processes can also be generated by protein crowding [Stachowiak et al., 2012] and steric pressure applied by intrinsically disordered domains of membrane-bound proteins [Busch et al., 2015]. Accumulation of cargo molecules on the outer surface of the plasma membrane promotes curvature generation and is expected to confront the endocytic machinery [Stachowiak et al., 2013, Kozlov et al., 2014]. It is proposed that a balance of steric pressure on the two surfaces of the membrane defines the final degree of curvature [Busch et al., 2015].

Curvatures with larger radii are generated via reorganisation of cortical actin cytoskeleton for a plethora of cellular functions, including cell migration (e.g., filopodia, lamellipodia and podosome formation), membrane trafficking (various endocytic pathways and exocytosis) and cytokinesis. In this mechanism, cortical actin filaments attached to membrane-bound proteins are responsible for pushing and/or pulling the membrane bilayer. This reorganisation is regulated by a series of signals including Wiskott–Aldrich syndrome protein (WASP) [Derry et al., 1994], WASP-family verprolin- homologous protein (WAVE) [Miki et al., 1998] and WAVE family proteins that activate actin-related protein-2/3 (Arp2/3) complex to lead actin polymerisation and subsequent membrane curvature formation [Takenawa and Miki, 2001, Takenawa and Suetsugu, 2007]. In the case of

CME, actin polymerisation is involved as an additional force to overcome membrane tension for transitioning the coat from U-shaped pits to Ω-shaped buds [Boulant et al., 2011]. Coarse-grained simulations predict such a transition to take place spontaneously under physiological membrane tension levels [Walani et al., 2015, Hassinger et al., 2017]. Whereas increased tension necessitates a combination of actin polymerisation and increased coat rigidity for vesicle budding [Hassinger et al., 2017]. In yeast cells, actin is required to counter turgor pressure during formation of endocytic vesicles [Aghamohammadzadeh and Ayscough, 2009, Galletta et al., 2010]. However, actin is dispensable for CME in mammalian cells and required only upon increased membrane tension during mitosis [Kaur et al., 2014], at the apical surface of polarised cells [Boulant et al., 2011, Hyman et al., 2006], and due to mechanical manipulations of the cell membrane [Ferguson et al., 2017]. Cargo with large sizes and stiffnesses also necessitate actin polymerisation for clathrin-mediated internalisation [Jain et al., 2019, Thottacherry et al., 2018, Doherty and McMahon, 2009, Cureton et al., 2010].

To conclude, cells harness a multitude of mechanisms to alter and adjust membrane curvature. The magnitude of local membrane tension regulates the energetics of curvature generation. Therefore, heterogeneity in stoichiometry and dynamics of curvature generating proteins are dictated by variations in local membrane tension [McMahon and Gallop, 2005, Farsad and Camilli, 2003, Antonny, 2011, Jarsch et al., 2016]. This tight link between membrane tension and membrane curvature generation is a key factor in endocytosis.

Mechanoregulation of CME

The dynamic interplay between membrane tension and curvature generation plays key roles in a variety of physiological functions including endocytosis. Endocytosis is a central cellular process that mediates active transport of various cargo molecules, such as transmembrane proteins and their extracellular ligands, nutrients and pathogens from the plasma membrane to the cytoplasm. Eukaryotic cells employ multiple endocytic pathways to regulate a wide range of cellular processes and cell homeostasis. The impairment of endocytic entries is implicated in diseases like cancer, neurodegeneration, muscle defects, immunological disorders and lysosomal storage diseases [Yarwood et al., 2020].

Endocytic processes are tightly coupled to cellular mechanics [Joseph and Liu, 2020, Thottacherry et al., 2018] and involve dynamic and extensive protein-mediated remodelling of the local cellular membrane to generate nanoscale invaginations that eventually mature into vesicles or tubules. As discussed in the previous section, remodelling of the plasma membrane is dictated by the molecular and mechanical features of the membrane. For successful generation of vesicles, endocytic machinery should be able to generate forces to overcome membrane tension [Boulant et al., 2011]. Therefore, the tension level on membrane and efficiency of endocytosis are inversely correlated [Ferguson et al., 2016, Willy et al., 2017]. Recent advancements in cellular scale imaging and force measurement/manipulation techniques have revolutionised the understanding of mechanoregulation of different endocytic pathways including phagocytosis, pinocytosis, CME or caveolin-mediated endocytosis, and CLIC/GEEC (clathrin-independent carriers/glycosylphosphotidylinositol-anchored protein-enriched compartments) endocytic pathways.

Over the past decades, advancements in live-cell imaging, biochemical techniques, and microscale mechanical manipulations of the cellular membrane unveiled a comprehensive understanding of endocytic clathrin coat formation and revealed that CME dynamics are tightly linked to membrane mechanics (Figures 1D–1F). In this section, we will discuss how CME dynamics within cells and tissues are regulated by the mechanical states of the plasma membrane, particularly by membrane tension. For a comprehensive understanding of the mechanoregulation of CME dynamics, we will first introduce the experimental techniques and analytical metrics utilised to quantify it. We will then expound on systematic spatiotemporal regulation of CME dynamics during central cellular processes.

Assessing CME dynamics in living cells and tissues

EM images of purified coated vesicles [Pearse, 1975, Kanaseki and Kadota, 1969] and adherent surfaces of unroofed cells [Heuser, 1980] have revealed the nanoscale organisation and morphology of endocytic

clathrin-coated structures. However, due to the lack of a temporal component, EM snapshots cannot reveal the dynamics of processes that give rise to formation of endocytic complexes [Willy et al., 2019]. Quantification of CME dynamics depends on real-time visualisation of fluorescently tagged clathrin coat components (Figure 1). High magnification epifluorescence [Gaidarov et al., 1999], spinning disk confocal fluorescence [Ehrlich et al., 2004] and total internal reflection fluorescence (TIRF) microscopy [Merrifield et al., 2002, Cocucci et al., 2012] techniques have allowed researchers to monitor different stages of clathrin coat formation within live cells. However, the optical resolution of these conventional imaging techniques is limited by diffraction of the fluorescence emission and, within the visible regime, cannot go beyond 200 nm. Therefore, clathrin coats, which are significantly smaller than this resolution limit, appear as diffraction-limited spots regardless of the density and spatial distribution of their fluorescent tags (Figures 1G and 1H) [Kural and Kirchhausen, 2012].

Time-lapse fluorescence imaging of live cells enables monitoring formation and internalisation of individual endocytic clathrin coats [Kural and Kirchhausen, 2012]. Formation of an endocytic coat is marked by the appearance of a diffraction-limited fluorescence spot that increases in intensity continuously due to accumulation of fluorescently tagged clathrin coat components. This spot disappears gradually as the coat disassembles due to the uncoating reaction or moves out of the focal plane (Figures 3A and 3B) [Ehrlich et al., 2004, Ferguson et al., 2016, Massol et al., 2006]. Single particle tracking algorithms are employed for accurate detection and tracing of all clathrin coat images within fluorescence microscopy acquisitions [Mettlen and Danuser, 2014, Kural et al., 2012, Jaqaman et al., 2008, Aguet et al., 2013, Aguet et al., 2016]. The lifetime of these traces (the time between coat assembly and disassembly) is a broadly used metric for characterisation of CME dynamics (Figure 3B). The effects of mechanical factors on clathrin coat assembly are often defined in terms of changes in distributions of clathrin coat lifetimes [Willy et al., 2017, Willy et al., 2019] (Figure 3C). Quantifying the lifetime distributions depend on accurate tracking of individual clathrin coats from initiation to dissolution, which is error-prone within high density particle fields and regimes with low signal-to-noise [Mettlen and Danuser, 2014]. Therefore, these conventional analytical approaches cannot be applied to cells within complex three-dimensional contexts, such as tissues [Ferguson et al., 2016].

Any factor that affects the formation and dissolution of clathrin coats during endocytic vesicle formation is a potential regulator of clathrin coat lifetime and hence, CME dynamics (Figure 3E). Therefore, the incorporation and dispersion rates of clathrin coat components can be used as an alternative quantitative reporter of CME dynamics [Ferguson et al., 2016]. To this end, formation (positive growth) and dissolution (negative growth) rates of individual clathrin coats can be deduced from short temporal windows within fluorescence microscopy assays and distributions compiled from these growth rates can be used to assess CME dynamics from acquisitions shorter than the mean clathrin coat lifetime. In other words, spatiotemporal changes in CME dynamics can be monitored in real time with less susceptibility to errors associated with particle detection and tracking as they can be derived from fragments of incomplete clathrin coat component traces [Ferguson et al., 2016].

The physical factors that elongate endocytic vesicle formation also reduce the formation and dissolution rates of clathrin-coated structures (Figure 3E). The high magnitude growth rates, that is, rapid changes in the clathrin signal corresponding to fast formation and dissolution of the coat, disappear upon introduction of energy barriers to vesicle formation [Ferguson et al., 2017] (Figure 3F). Consequently, the standard deviations (SDs) of the growth rate distributions drop (Figure 3G). Since such distributions can be assembled for each frame of a time-lapse acquisition, this approach enables real time monitoring of temporal changes in endocytic dynamics in response to rapid fluctuations in the mechanical state of cells and tissues. The rates of formation or dissolution can be constructed before the completion of traces, thus report changes in CME dynamics taking place within time scales shorter than mean clathrin coat lifetime [Ferguson et al., 2016, Ferguson et al., 2017] (Figures 3H and 3I). Such rapid changes in CME dynamics cannot be dissected by conventional clathrin coat lifetime analyses. In addition, determining clathrin coat lifetimes is error prone especially within live tissues where, due to the high density and motility of clathrin coats, single particle tracking is infeasible for the entire clathrin coat lifetime.

Figure 3 | Assessing endocytic clathrin coat dynamics

(**a**) Kymograph shows the CME activity at the ventral surface of a cell. Each dark streak is the trace of an individual clathrin coat. Blue and red arrowheads mark the initiation and dissolution of a clathrin coat, respectively, and the time between the two (Δt) is the lifetime. Clathrin traces elongate gradually upon increase of membrane tension via microaspiration of the cell from the dorsal surface (starting with the dashed line). (**b**) Fluorescence intensity profiles are shown for three independent endocytic clathrin coats with lifetimes of 105, 63 and 38 s, respectively. In each trace, increasing signal intensity is due to the growth/formation of the coat and the rapid dimming marks the dissolution (i.e., uncoating). (**c**) Microaspiration slows down CME dynamics due to increased tension. Clathrin coat lifetime distributions are assembled for cells before and during aspiration. (**d**) Density of *de novo* clathrin-coated vesicle formation also reduces significantly with the increasing levels of membrane tension. (**e**) Fluorescence intensity traces of multiple clathrin-coated structures are averaged after synchronisation at the beginning, maximum intensity frame and end of traces. Both the rates of growth/formation and dissolution slow down upon microaspiration. (**f**) Change in endocytic dynamics induced by increased tension (due to microaspiration) can be observed in growth rate distributions. Increasing tension inhibits fast formation and dissolution rates, resulting in distributions having smaller standard deviations (SDs). (**g**) The change in the SD of clathrin growth rates is shown for 9 microaspirated BSC1 cells. The lower SD values indicate slower CME dynamics. (**h**) Membrane tension can also be changed by increasing the hydrostatic pressure in cells upon squeezing. Kymograph shows the clathrin traces detected at the ventral surface of a cell at two distinct levels of squeezing (marked by the dashed lines). (**i**) The SD of the growth rates reduce in a stepwise manner due to increased membrane tension at discrete levels of squeezing. Reproduced, with permission, from Ferguson et al. (2016, 2017).

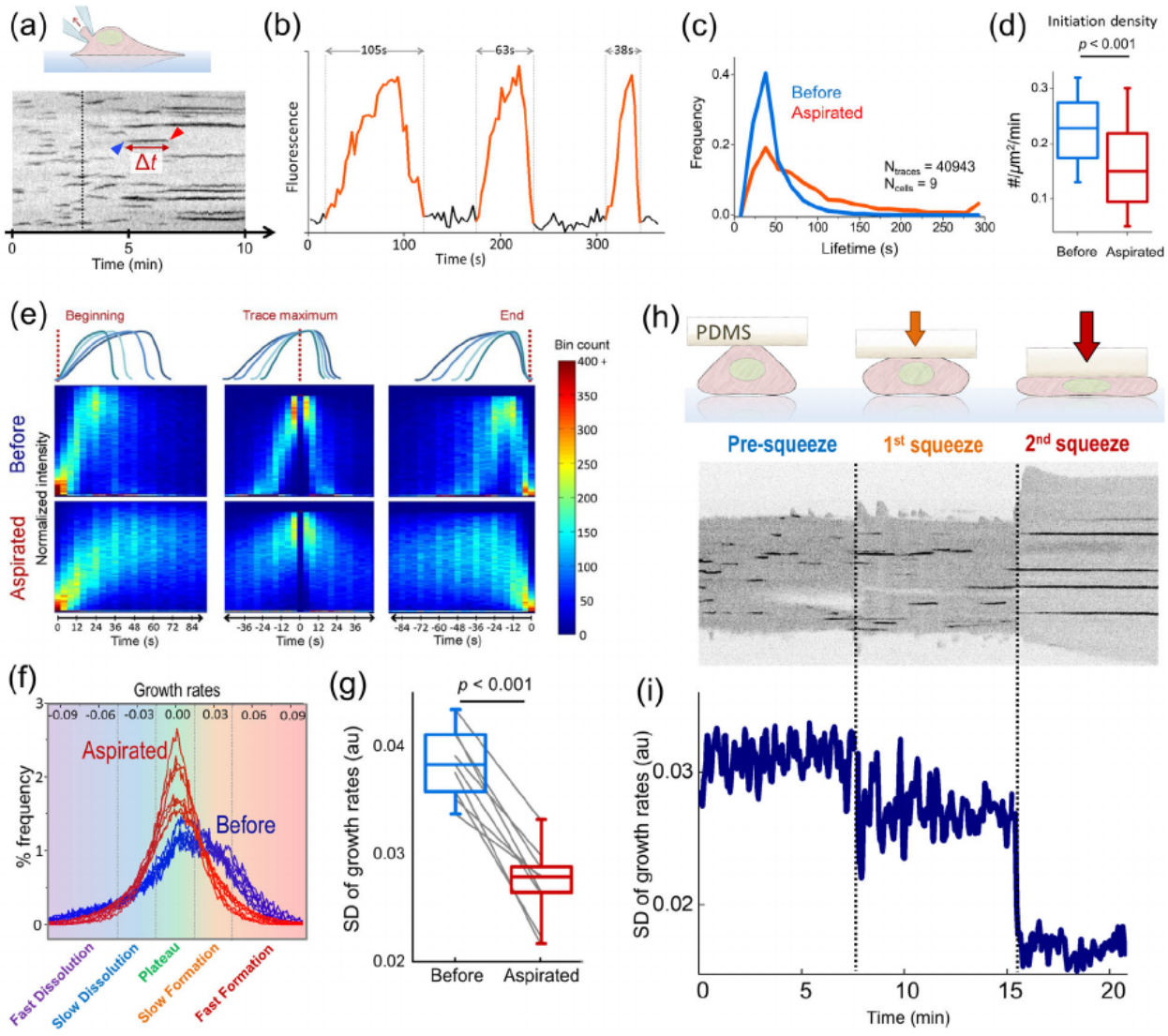

Figure 4 | Spatiotemporal variations in CME dynamics during *Drosophila* embryogenesis

(**a**) Changes in CME dynamics at the amnioserosa tissues during the dorsal closure of embryos. Box plots show SD of growth rate distributions obtained from amnioserosa tissues at early and late stages of the dorsal closure. CME dynamics slow down with increasing tension in the tissue. (**b**) Left, clathrin-coated structures at the dorsal surface of a *Drosophila* embryo. Right, SD map determined using clathrin growth rates obtained at the amnioserosa (AS) and the lateral epidermis (LE) tissues. Lower values of the SD demonstrate slower CME dynamics at the AS tissue. (**c**) More examples demonstrating the spatial heterogeneity of CME dynamics at the dorsal surface of late stage *Drosophila* embryos. (**d**) Box plots showing SD of growth rates obtained from lateral epidermis and amnioserosa tissues. Reproduced, with permission, from Willy et al. (2017).

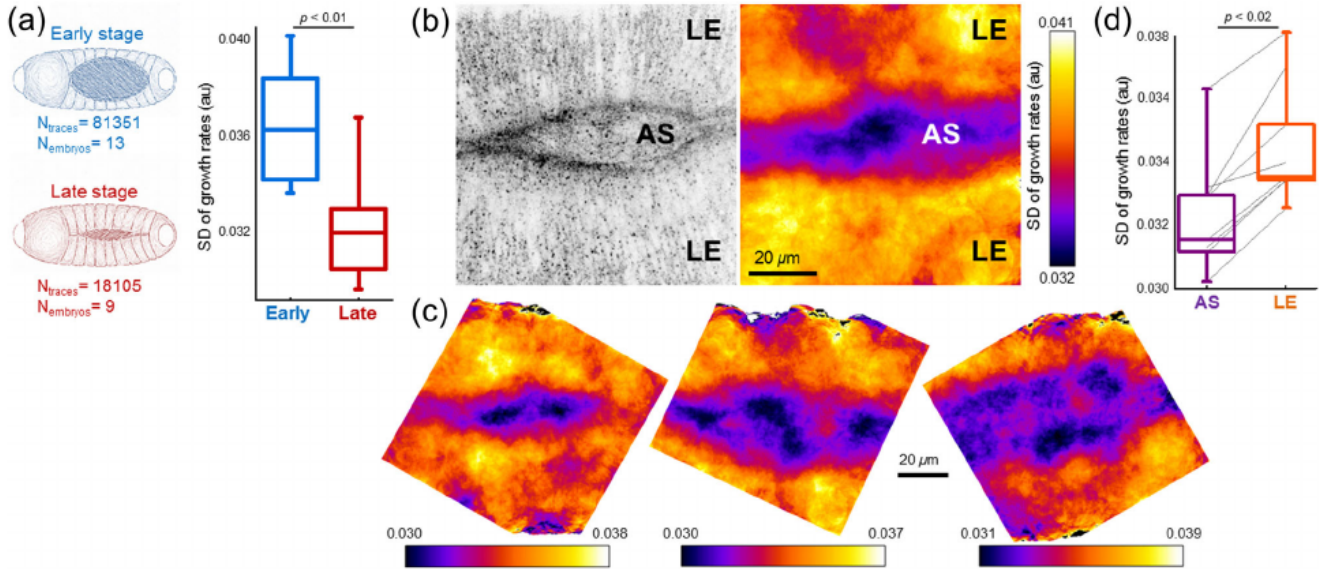

The efficacy of the two approaches was compared by monitoring the clathrin coat dynamics at the amnioserosa tissue of developing *Drosophila* embryos [Ferguson et al., 2016, Willy et al., 2017]. The lifetime distribution analysis showed that both basal and apical surfaces of amnioserosa are dominated by short clathrin signal traces, which are classified as abortive (non-endocytic) clathrin pits. In contrast with results derived by the lifetime distributions, the growth rate analysis of clathrin structures demonstrated that the apical surface is essentially dominated by less dynamic (longer-lived) pits. The observed short-lived structures are mainly the incomplete traces of clathrin coats that are artifacts of single particle tracking [Mettlen and Danuser, 2014]. These results exemplify that growth rate analysis is a more accurate alternative for quantifying CME dynamics within contexts where single particle tracking is error prone, such as tissues of multicellular organisms [Ferguson et al., 2016]. Growth rate analysis allowed detection of spatiotemporal changes in CME dynamics at the dorsal surface of developing *Drosophila* embryos [Ferguson et al., 2016, Willy et al., 2017]. Tension increase at the amnioserosa tissue throughout the dorsal closure results in slower clathrin coat formation and dissolution in later stages (Figure 4A) [Ma et al., 2009, Saias et al., 2015]. SD of clathrin coat growth rates obtained within small areas allows to generate maps that demonstrate spatial heterogeneity in CME dynamics (Figures 4B, 4C and 7C). Overall, CME dynamics are slower at the amnioserosa tissue with respect to the lateral epidermis around it (Figure 4D).

The shortcomings of conventional fluorescence imaging can be circumvented by super-resolution fluorescence live cell imaging techniques, which enable fast image acquisition (up to ~100 ms/frame) with spatial resolving significantly better than the diffraction-limited microscopy systems (20–100 nm) [Guo et al., 2018]. Among these techniques, structured illumination microscopy (SIM) (Figure 5A) [Willy et al., 2019, Fiolka et al., 2012, Li et al., 2015], stimulated emission depletion microscopy

Figure 5 | (**a**) TIRF–SIM time-lapse acquisitions in live COS-7 cells show clathrin-coated pits aggregated into plaques and dissociation of individual pits (indicated by arrowheads) from the plaque. Reproduced, with permission, from Li et al. (2015). (**b**) Three-dimensional stochastic optical reconstruction microscopy (STORM) images show a clathrin plaque at different axial positions. Arrowheads mark the positions of clathrin-coated pits in the vicinity of the plaque. Scale bar, 1 μm. Reproduced, with permission, from Leyton-Puig et al. (2017). (**c**) Generative adversarial networks enable super-resolution in clathrin coat images acquired using diffraction-limited microscopy. Clathrin-coated structures at the ventral surface a SUM159 cell genome edited to express AP2 adaptor protein fused with GFP, where the left panel is the original acquisition at the TIRF mode, the middle panel is the TIRF–SIM image of the same area, and the right panel is the prediction of the deep neural network. The intensity profile between the two arrowheads is plotted at the bottom-right corner of each image to demonstrate resolution enhancement. Scale bar, 500 nm. Reproduced, with permission, from Wang et al. (2019).

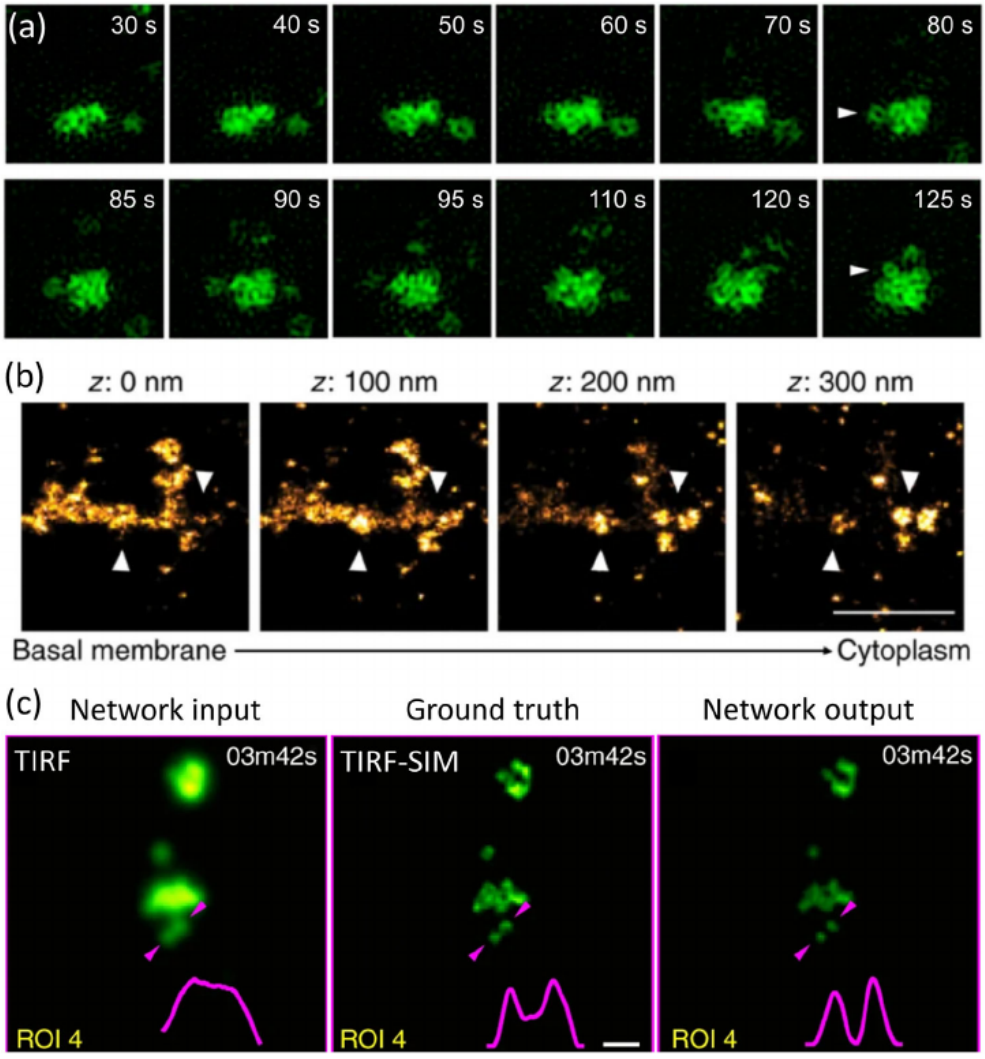

[Bianchini et al., 2015, Almeida-Souza et al., 2018], single molecule localisation-based techniques (Figure 5B) [Jones et al., 2011, Leyton-Puig et al., 2017] and lattice light-sheet microscopy [Kural et al., 2015, Chen et al., 2014, Schöneberg et al., 2018, Liu et al., 2018] are commonly employed for imaging clathrin-coated structures with high spatiotemporal resolution and low phototoxicity. A recently developed alternative is the use of deep neural networks for increasing the spatial resolution of live cell images obtained using various diffraction-limited microscopy applications. Wang et al. (2019) have

recently shown that generative adversarial networks can be trained to transform clathrin coat images obtained using conventional fluorescence imaging to the equivalents of super-resolution microscopy acquisitions (Figure 5C).

Noncanonical clathrin-coated structures

Fluorescence microscopy applications have revealed that not all clathrin coats mature into endocytic vesicles [Willy et al., 2017, Kirchhausen et al., 2014, Hong et al., 2015, Loerke et al., 2009]. Three dynamically disparate populations of clathrin-coated structures with distinct lifetime modes are observed: abortives, pits and plaques [Saffarian et al., 2009, Loerke et al., 2012, Grove et al., 2014, Lampe et al., 2016]. Among these populations, clathrin-coated pits (also referred as canonical-coated pits [Kirchhausen, 2009]) are believed to bear the majority of the endocytic load.

The majority of clathrin coats fail to mature into pits and disassemble without generating endocytic vesicles [Ehrlich et al., 2004, Kirchhausen, 2009]. These 'abortive' coats are small and short-lived structures that make up a large fraction of clathrin coats detected in fluorescence acquisitions [Taylor et al., 2011, Tan et al., 2015, Liu et al., 2009]. Their proposed function is a proof-reading mechanism to ensure that endocytic vesicles are not internalised without cargo [Chen et al., 2019, Vanden Broeck and De Wolf, 2006]. In addition to absence of cargo, factors that prevent clathrin coat stabilisation on plasma membrane trigger early dissolution of the coat. Particularly, depletion of clathrin coat components [Vanden Broeck and De Wolf, 2006, Kadlecova et al., 2017] and significant elevation in membrane tension prevents initiation of canonical clathrin pits (Figures 1F and 3D) [Willy et al., 2017]. Recent works revealed that short-lived clathrin-coated structures can act as platforms for EGF-induced signalling [Rosselli-Murai et al., 2018]. In addition, a molecularly distinct sub-population of clathrin pits, smaller in size and faster in internalisation than clathrin pits utilising AP2 adaptors, is implicated in EGFR internalisation and degradation [Pascolutti et al., 2019].

The other subpopulation of clathrin-coated structures are plaques, which are structurally and dynamically different from clathrin pits [Baschieri et al., 2020]. Plaques are extended flat clathrin lattices with longer lifetimes compared with coated pits [Kirchhausen et al., 2014] (Figure 1A). Plaques are found mostly at the ventral/adherent surfaces of cultured cells in the proximity of substrate adhesion sites [Ferguson et al., 2016, Maupin and Pollard, 1983, Batchelder and Yarar, 2010]. Their prevalence in cultured cells depends on a multitude of factors including alternative splicing of clathrin heavy chain [Moulay et al., 2020], expression levels of AP2 adaptors [Dambournet et al., 2018], hypotonic swelling [Heuser, 1989], substrate rigidity [Baschieri et al., 2018] and strength of cell adhesion sites [Batchelder and Yarar, 2010, Heuser, 1989, Akisaka and Yoshida, 2021]. Recent studies showed that plaques can be found in living tissues and non-adherent cells as well [Grove et al., 2014, Vassilopoulos et al., 2014, Franck et al., 2019, Bellve et al., 2006]. The clathrin plaques are characterised as endocytic structures that fail to overcome local mechanical obstructions in order to form an invagination or elongate the invagination for vesicle formation [Ferguson et al., 2016, Saffarian et al., 2009]. Under high tension, clathrin-coated structures can experience a delay in curvature generation and subsequent vesicle formation, which leads to an overall increase in clathrin lifetime. Thereby, an increase in tension favours formation of plaques [Ferguson et al., 2016, Willy et al., 2017, Saleem et al., 2015, Heuser, 1989, Bucher et al., 2018] and, consequently, the spatial diversity in the density of plaques is dictated by variations in substrate adhesion and local membrane tension [Baschieri et al., 2018, Zuidema et al., 2018] (Figure 1E).

There is a significant discord in the literature related to the origin and function of clathrin plaques. Although plaques are observed as homogenous patches of flat clathrin lattices in EM images [Heuser, 1989], under super-resolved fluorescence imaging, plaques may appear as aggregates of clathrin pits, occasionally detaching from edges of the plaque (Figures 5A and 5B) [Li et al., 2015]. Several findings suggest that plaques have non-endocytic functions related to cell adhesion and signal transduction [Grove et al., 2014, Batchelder and Yarar, 2010, Vassilopoulos et al., 2014, Franck et al., 2019, Bellve et al., 2006, Lock et al., 2018, Liu et al., 2019]. It is also proposed that plaques as a whole do not mature into vesicles but are employed as structural imprints, that is, hotspots on the membrane for

multiple rounds of new endocytic coat formation [Lampe et al., 2016] (Figures 5A and 5B).

Some studies concluded that pits and flat clathrin lattices are independent endocytic structures [Saffarian et al., 2009], whereas others claim that flat lattices are prerequisites of pits and subsequent endocytic vesicle formation [Avinoam et al., 2015, Bucher et al., 2018]. This brings us to an ongoing controversy regarding curvature generation during formation of clathrin-coated pits. On one extreme of the spectrum, it is proposed that curvature of the clathrin coat is constant during its entire lifetime. According to this model, clathrin directly polymerises into a curved lattice on the membrane (Figure 1B) [Kirchhausen, 2009, Willy et al., 2019, Saffarian et al., 2009, Chen et al., 2019, Cocucci et al., 2012, Narasimhan et al., 2019]. The alternative model suggests that clathrin initially assembles into a flat lattice and then rearranges into a spheroid via transformation of some hexagonal faces into pentagons, while keeping its surface area constant (Figure 1C). This model is based on EM studies, where both flat lattices and curved structures were observed and arranged into a temporal order [Heuser, 1980, Avinoam et al., 2015, Sochacki and Taraska, 2019, Bucher et al., 2018].

Owing to enhanced resolution in both spatial and temporal domains, super-resolved fluorescence imaging performed within live cells and tissues have provided important insights regarding curvature generation by clathrin-coated pits forming *de novo* [Willy et al., 2019]. However, in these studies, the spatial resolution is still not adequate to perform the same analysis on clathrin pits that seem to be detaching from plaques (Figure 5A). Outstanding questions include whether these pits originate from flat patches at the edges of plaques [Lampe et al., 2016], as predicted by coarse-grained simulations [Den Otter and Briels, 2011], or if they are *de novo* structures that happen to form in the vicinity of an aggregate of pits [Li et al., 2015].

Spatiotemporal regulation of endocytic clathrin coat dynamics by membrane tension

CME dynamics are tightly linked to tension on the plasma membrane. Tension resists membrane deformation and invagination during endocytic clathrin coat assembly. Plasma membrane tension of adherent cells is not uniform and is a combination of in-plane tension, and membrane–cytoskeleton and membrane-substrate adhesions, which are spatially heterogeneous throughout the cell [Lieber et al., 2015, Diz-Muñoz et al., 2013, Batchelder and Yarar, 2010, Dai and Sheetz, 1995, Le Roux et al., 2019]. Accordingly, local variations in tension induce spatial and temporal heterogeneity in the lifetime, curvature, stability and distribution of clathrin coats (Figure 1B and 1C) [Kural et al., 2015, Ferguson et al., 2017, Willy et al., 2017, Aguet et al., 2016, Tsujita et al., 2015]. Removal of mechanical hindrances restores the structural and dynamic features of clathrin-coated structures [Ferguson et al., 2017, Willy et al., 2017, Saleem et al., 2015]. Overall, the current understanding of the mechanoregulation of CME dynamics is built on a multitude of approaches that utilise *in vitro* reconstitution systems [Saleem et al., 2015, Brod et al., 2020, Meinecke et al., 2013, Purushothaman and Ungermann, 2018, Steinem and Meinecke, 2020], computational simulations [Hassinger et al., 2017, Walani et al., 2015, Agrawal et al., 2010, Irajizad et al., 2017, Giani et al., 2017, Giani et al., 2016, Mahmood et al., 2019] and live-cell imaging assays that incorporate tension manipulation on the membrane [Ferguson et al., 2016, Willy et al., 2017].

In-plane tension on the plasma membrane can be modified globally, often reversibly, via mechanical and biochemical manipulations. These techniques include alterations of lipid and cholesterol compositions of the plasma membrane [Willy et al., 2017, Riggi et al., 2019], changes in osmolarity within a cell [Diz-Muñoz et al., 2016], cell stretching [Boulant et al., 2011, Thottacherry et al., 2018], microaspiration and compression [Ferguson et al., 2017], all of which are compatible with fluorescence live-cell imaging modalities. Real-time manipulations of mechanical stimuli within live cells showed that plasma membrane tension is a fast-acting and effective regulator of CME [Ferguson et al., 2017, Willy et al., 2017]. Overall endocytic vesicle formation is slowed down by increased tension as it resists the generation of curved clathrin coats [Ferguson et al., 2016, Saleem et al., 2015, Gauthier et al., 2011, Apodaca, 2002, Gauthier et al., 2012]. Conversely, decreasing the tension increases endocytic rates [Saleem et al., 2015, Raucher and Sheetz, 1999], enabling CME machinery to generate curvature upon a reduced energy barrier. Incremental

changes in plasma membrane tension yield an immediate effect on CME dynamics. Elevation of membrane tension via micropipette aspiration and increase in hydrostatic pressure via cell squeezing or hypotonic swelling increase the mean lifetime of clathrin coat structures, and correspondingly reduce the SD of growth rate distributions as well as surface density of clathrin coat initiation and conclusion events (Figure 3). Relieving the tension restores CME dynamics by reducing clathrin coat lifetimes and increasing the SD of growth rates [Ferguson et al., 2017].

Changes in tension induced by mechanical and chemical manipulations are kept within boundaries of mechanical forces utilised in cellular and morphogenetical processes [Ferguson et al., 2017]. Recent advancements in deep tissue imaging modalities augmented the understanding of the systems level interplay between membrane tension and CME dynamics within physiological contexts [Ferguson et al., 2016, Willy et al., 2017, Willy et al., 2019, Aguet et al., 2016, Schöneberg et al., 2018, Liu et al., 2018]. As we discuss in the next section, physiological processes like cell adhesion, spreading, migration, division and development of multicellular organisms generate spatial and temporal variations in membrane tension [Lieber et al., 2015, Fogelson and Mogilner, 2014] which results in heterogeneity of endocytic clathrin coat lifetimes, curvature and distribution [Kural et al., 2015, Ferguson et al., 2016, Ferguson et al., 2017, Willy et al., 2017, Aguet et al., 2016, Lock et al., 2018].

The interplay between tension and CME during physiological processes

Cellular processes associated with changes in cell morphology, such as spreading, division and migration, require significant transformations at the peripheral regions of the cell, which include reconfiguration of the (i) cytoskeletal cell cortex, (ii) density and dynamics of cytoskeleton-membrane adhesion sites and (iii) size, density and molecular composition of membrane–substrate adhesion sites. All these factors, along with changes in the volume-to-surface-area of the cell, result in spatiotemporal heterogeneity in the apparent membrane tension and, thereby, membrane trafficking pathways, including CME (Figures 1C and 1C).

Cell spreading

Spreading is one of the first interactions that a cell makes with its substrate, where cell–substrate contact area increases by swift changes in focal adhesion recruitment, adhesion receptor binding and actin polymerisation [Reinhart-King et al., 2005]. A cell typically adheres to a surface via receptor-ligand binding, followed by extension of filopodia away from the cell body [Sens and Plastino, 2015]. The cell then leaves its rounded morphology and transitions to a flattened state [Ng et al., 2019], as additional bonds are formed through actin cytoskeletal rearrangements that structure into focal adhesions and interact with the substrate (Figures 8A–8D) [Reinhart-King et al., 2005]. Achieving efficient cell spreading requires spatiotemporal variations in membrane tension, which propagates along the plasma membrane, in order to compensate for the energy required to instigate these processes [Tsygankova and Keen, 2019] and to maintain an overall tension steady state across the cell (Figure 2G) [Willy et al., 2017, Gauthier et al., 2009, Gauthier et al., 2011].

Several factors contribute to tension heterogeneity during cell spreading. Actin cytoskeleton polymerisation pushes the plasma membrane away from the cell body anisotropically [Reinhart-King et al., 2005], which generates forces against rising membrane tension caused by the diminishing amount of area from unfolding plasma membrane folds (Figures 6A and 8B) [Gauthier et al., 2012, Masters et al., 2013]. Increased tension is immediately followed by activation of exocytosis and myosin activity, just as the cell begins to contract [Gauthier et al., 2011] and generates additional tension on newly assembling focal adhesions [Parsons et al., 2010] (Figure 8C). These focal adhesions subsequently attach and exert forces on the substrate as the plasma membrane simultaneously increases in area and decreases in tension [Gauthier et al., 2012]. At this point, the asymmetric profile of the spreading cell becomes apparent [Rangamani et al., 2011], as membrane tension stabilises due to a reduction in actin-induced protrusions and retractions. Further, exocytosis activity is counteracted by endocytic processes to maintain a constant plasma membrane area [Gauthier et al., 2012] (Figure 8D). CME in particular, experiences temporal heterogeneity alongside spatial fluctuations in cell membrane tension, as the average

Figure 6 | CME dynamics in spreading cells

(**a**) Membrane tether force measurements conducted on a spreading cell demonstrate increased tension during extension of the membrane and reduction in tension during retraction. Yellow dashed line shows the position of the cell boundary over time. Reproduced, with permission, from Masters et al. (2013). (**b**) Snapshots show the bottom surface of a spreading cell at different time points. Note that clathrin coat initiation is hindered due to high membrane tension at the early stages of spreading (see Figure 2G). Traces with distinct colours belong to endocytic clathrin coats with different lifetimes. (**c**) For the spreading cell shown in *b*, the upper panel shows the change in average clathrin coat lifetime and spreading area. The bottom panel is the temporal evolution of the SD of growth rates during spreading. Note that increased clathrin lifetimes and reduced SD mark slow CME dynamics due to high tension during spreading. The dynamics recover when the spreading is complete. (**d**) Average normalised lifetime is plotted for different membrane extension rates obtained from multiple spreading cells. Reproduced, with permission, from Willy et al. (2017).

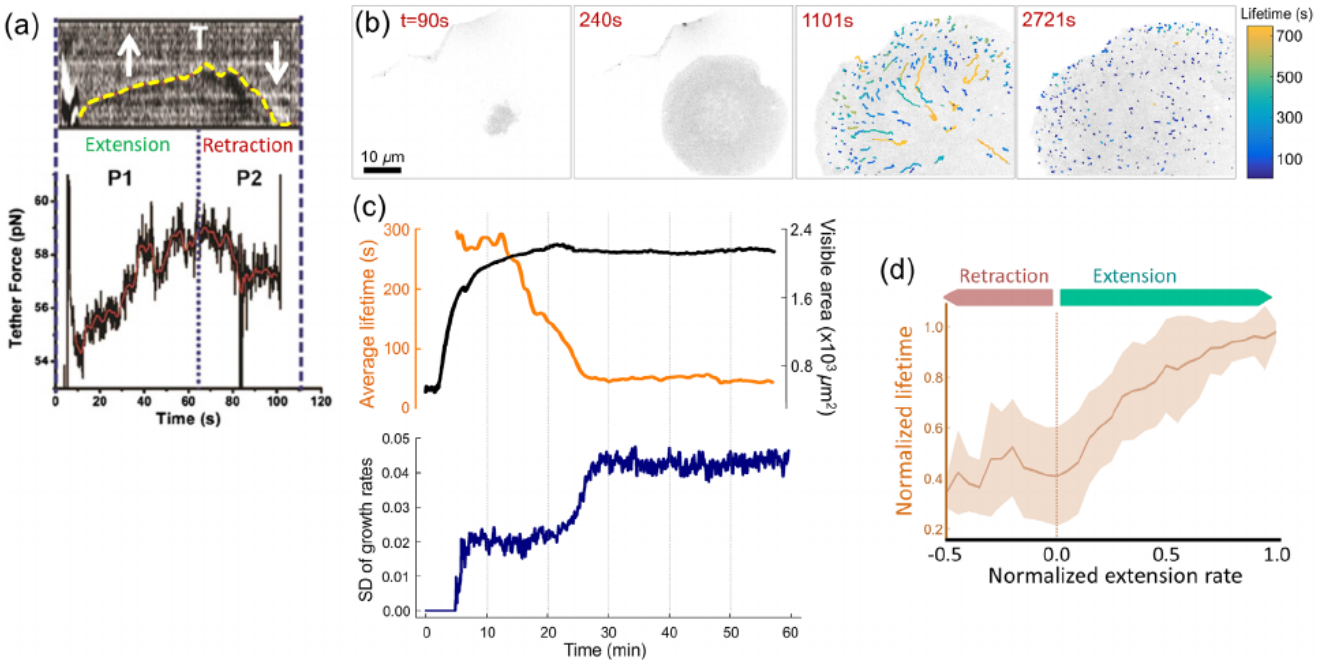

lifetime of clathrin coats is increased upon expansion of cell spreading area and is decreased upon interruption of expansion [Willy et al., 2017] (Figures 6B–6D). Though spatial heterogeneity in CME dynamics has also been documented (Figure 1C) [Willy et al., 2017], further studies on probing clathrin coat dynamics at discrete areas of spreading cells are necessary for a more comprehensive understanding of the roles of CME in facilitating cell shape changes during spreading.

Cell division

After completion of cell division, daughter cells adhere to substrate and start spreading until a critical size is reached. After this point, membrane–substrate and membrane–cytoskeleton adhesions have regulatory roles in progression throughout the cell cycle stages. Disruption of cell adhesion by chemical or physical factors can trigger cell cycle arrest [Margadant et al., 2013, Walker et al., 2005], which can inhibit cell growth and restrict adhesion-mediated spreading [Huang et al., 1998, Gérard and Goldbeter, 2014]. Reciprocally, cell adhesion states change in a cell cycle-dependent manner [Jones et al., 2018, Théry and Bornens, 2006]. At the onset of mitosis, the cell disconnects from the substrate and rounds up again to prepare for scission into two daughter cells [Legoff and Lecuit, 2016]. Membrane tension is the highest at this stage of the cell cycle due to the increased cell volume-to-surface-area ratio [Raucher and Sheetz, 1999, Stewart et al., 2011]. Indeed, early work in the field revealed that

clathrin-mediated uptake of specific ligand molecules (transferrin and LDL) is inhibited during mitosis [Raucher and Sheetz, 1999, Pypaert et al., 1991, Sager et al., 1984, Oliver et al., 1985]. Conversely, induced reduction of membrane tension during mitosis leads to an increase in endocytosis rates [Raucher and Sheetz, 1999].

The mechanism proposed for inhibition of CME during mitosis is the repurposing of available G-actin into the process of membrane constriction [Kaur et al., 2014], and thereby, actin polymerisation cannot support clathrin-mediated cargo internalisation at elevated levels of tension [Boulant et al., 2011]. A shortcoming of these assays is that bulk cargo internalisation assays can only report cumulative and ensemble-averaged effects on endocytic rates, and thus are not suitable for precise assessment of CME dynamics. Studies utilising single cell analysis later reported that CME dynamics are steady throughout the cell cycle phases [Bitsikas et al., 2014, Boucrot and Kirchhausen, 2007], except during metaphase [Aguet et al., 2016]. Inhibition of cargo uptake is proposed to occur due to a decrease in the availability of receptors on the cell surface instead of inhibition of endocytic machinery [Boucrot and Kirchhausen, 2007, Tacheva-Grigorova et al., 2013]. Additionally, reduced internalisation and clathrin coat dynamics are shown to occur only when cells are chemically arrested at mitosis [Tacheva-Grigorova et al., 2013], which disrupts cytoskeletal organisation. In later experiments, mitotic cells are compared with cells in interphase, assuming that endocytic rates are similar throughout this phase. However, apart from a cell cycle-dependent abundance of cargo receptors, the G1, S and G2 stages of interphase display a non-homogeneous adhesion state [Heng and Koh, 2010] and membrane tension, which collectively affect endocytic rates. In addition, several cargo molecules are exclusively internalised during distinct stages of cell cycle [Snijder et al., 2009, Majoul et al., 2002, Liu et al., 2011, Fielding and Royle, 2014]. Cells favour migration, the process which requires extensive tussle with membrane tension, during particular stages of interphase in a context-dependent manner [Bonneton et al., 1999, Esmaeili Pourfarhangi et al., 2018, Krause et al., 2019]. Therefore, it is still not clear whether CME dynamics are stationary throughout the cell cycle or regulated in a cell cycle-dependent manner.

Our current understanding of CME comes largely from experiments conducted on cells in interphase. However, even monoclonal cells at various stages of interphase exhibit considerable variations in CME dynamics. One attractive hypothesis is that the heterogeneity in membrane tension during the cell cycle contributes to spatiotemporal regulation of CME dynamics. Indeed, we found that CME dynamics are inversely correlated to changes in membrane tension across different stages of interphase (unpublished data). The SD of clathrin growth rates is elevated as cells approach the G1 restriction point, where immense internalisation of extracellular growth signals is required for transition into S phase. We also found that during the cell cycle, a reduction in substrate contact area stimulates an increase in clathrin plaque density, which is in good agreement with previous reports [Tan et al., 2015]. The plaque density peaks during mitosis, where membrane tension is the highest. Indeed, a recent study discovered long-lived plaque-like structures in mitosis phase, which mediate dynamic cell adhesion during division and facilitate re-spreading of daughter cells [Lock et al., 2018]. These findings indicate that alterations in membrane tension may contribute to progression of the cell cycle via regulating CME dynamics.

Cell migration: solo and collective

Cell migration shares the same initial set of events with cell spreading but, beyond adhesion and protrusion, is additionally characterised by polarisation of the actin cytoskeleton to generate a single stable protrusion at the leading edge [Gauthier et al., 2012] (Figure 7A), as well as traction at the leading edge and detachment of the trailing edge from the substrate to move the cell body forward [Mitchison and Cramer, 1996]. Moreover, spatiotemporal heterogeneity of CME is manifested in the presence of tension gradients at the plasma membrane, which further has roles in maintaining directional cell migration.

In motile cell types, the establishment of a front-to-rear tension gradient has been exhibited along the plasma membrane in the direction of cell migration [Lieber et al., 2015, Fogelson and Mogilner, 2014]. Membrane tether measurement experiments have revealed a tension asymmetry between the leading and trailing edge of migrating keratocytes created by the establishment of actin polymerisation

Figure 7 | CME dynamics during cell migration

(**a**) Fluorescence image (inverted) shows clathrin-coated structures at the ventral and dorsal surfaces of a migrating cell. The arrow marks the direction of migration. (**b**) Clathrin coat traces obtained from the cell in *a* are colour coded relative to their z-position. (**c**) Growth rate map of the dorsal surface created using the SD of local clathrin growth rates. SD values are lower in the vicinity of the leading edge due to slower CME dynamics. (**d**) Lifetime distributions of dorsal clathrin coats at the lamellar region (orange) and leading edge (indigo). (**e**) Box plots show SD of growth rate distributions of clathrin coat populations at the leading edge and lamellar regions obtained in different cells. (**f**) Hemocytes expressing fluorescently tagged clathrin (green) and CD4 (red) are imaged at the ventral surface of late *Drosophila* embryos. For this particular hemocyte, the analyses in G–J demonstrate that the density of endocytic clathrin-coated structures is lower at the leading edge during *in vivo* migration. (**g**) Positions of the clathrin coats within the proximity of the cell surface are shown with green dots. (**H and I**) Gray scale represents thickness of the hemocyte. Z-position (**h**) and local densities (**i**) of clathrin-coated structures are colour coded. (**j**) Spatial density map of clathrin-coated structures generated from average distance between them. Reproduced, with permission, from Willy et al. (2017).

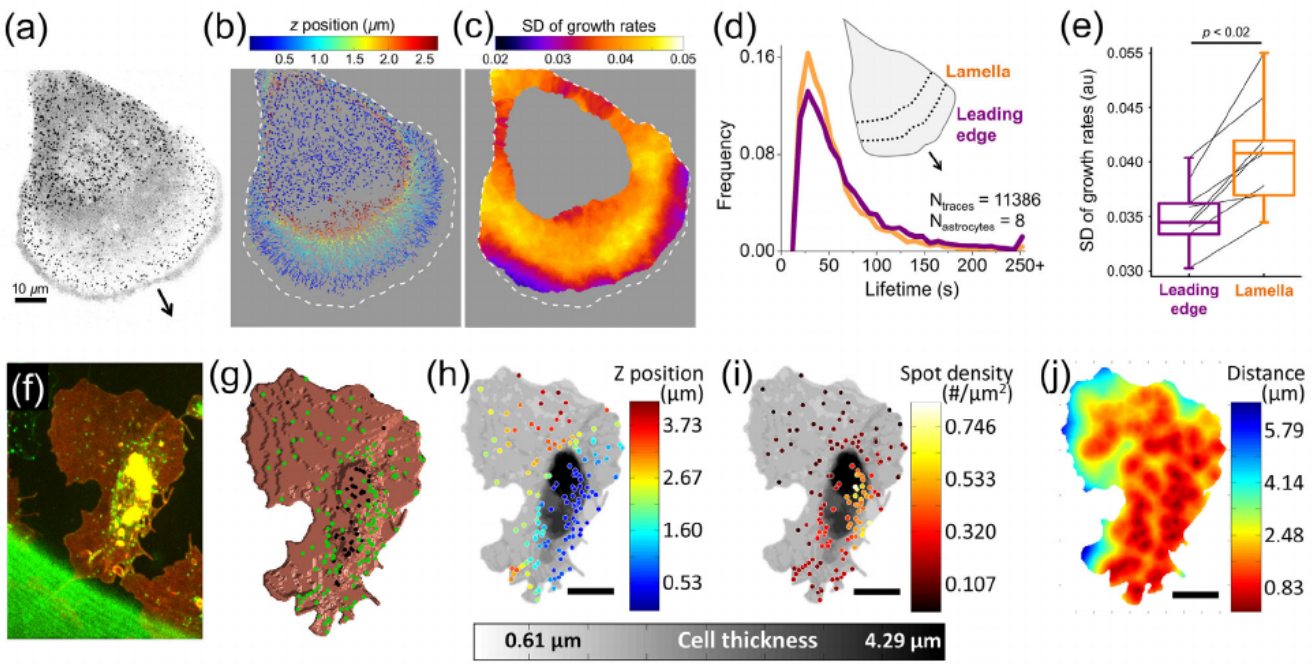

sites that lead the cell toward the direction of migration (Figure 2H) [Lieber et al., 2015]. Tension asymmetry regulates actin polymerisation, namely, to spatially decrease in density from the leading edge towards the lateral sides and trailing edge of a migrating cell, by allowing a competition between protrusive sites [Diz-Muñoz et al., 2016]. In effect, this competition creates a global negative feedback loop, where high membrane tension at the leading edge causes a cell to combine protrusions at this end and quickly inhibit protrusions at other locations [Houk et al., 2012, Kozlov and Mogilner, 2007] to improve cell polarisation, and thus enhance motility [Sens and Plastino, 2015, Diz-Muñoz et al., 2016]. Membrane curvature-sensing proteins, in particular, FBP17 (formin binding protein 17) has been shown to contribute to this negative feedback mechanism by localising at non-endocytic invaginations at the leading-edge protrusion of migrating cells to stabilise actin assembly, which leads to increased tension [Tsujita et al., 2015]. Migrating cells regulate tension-induced polarity by spatially confining the assembly of the actin cytoskeleton to promote directional migration.

It is also proposed that migrating cells make use of membrane trafficking to maintain polarity [Bretscher, 2008]. An inverse relationship occurs between CME dynamics and membrane tension in

Figure 8 | Origins of tension heterogeneity across the plasma membrane of spreading and migrating cells
(**a**) When newly placed on a substrate, the cell appears rounded and membrane tension is localised at membrane folds. (**b**) Isotropic spreading occurs as extra membrane is unfolded. Tension rises at locations of actin cytoskeleton polymerisation and as additional area provided by membrane folds is depleted. (**c**) Anisotropic spreading occurs, where focal adhesions are formed from actin rearrangement. Exocytosis levels increase to balance the high membrane tension manifested in isotropic spreading. (**d**) Plasma membrane area dramatically increases as the cell reduces the number of protrusions. Focal adhesions attach tightly to the substrate and tension stabilises towards a resting level, as cell spreading completes. Exocytosis activity is balanced by CME, which experiences spatiotemporal heterogeneity upon spreading. (**e**) Cell polarisation occurs due to rearrangement of the actin cytoskeleton, which results in the generation of a single stable protrusion at the leading edge and multiple protrusions at the trailing edge. A front-to-rear tension heterogeneity in the plasma membrane is exhibited [Lieber et al., 2015], where CME activity is reduced at the leading edge and enhanced at the trailing edge [Willy et al., 2017]. (**f**) Cell polarity is improved by adhesive contacts between the cell and the substrate. The establishment of a front-to-rear tension gradient generated by cell polarisation induces migration to occur.

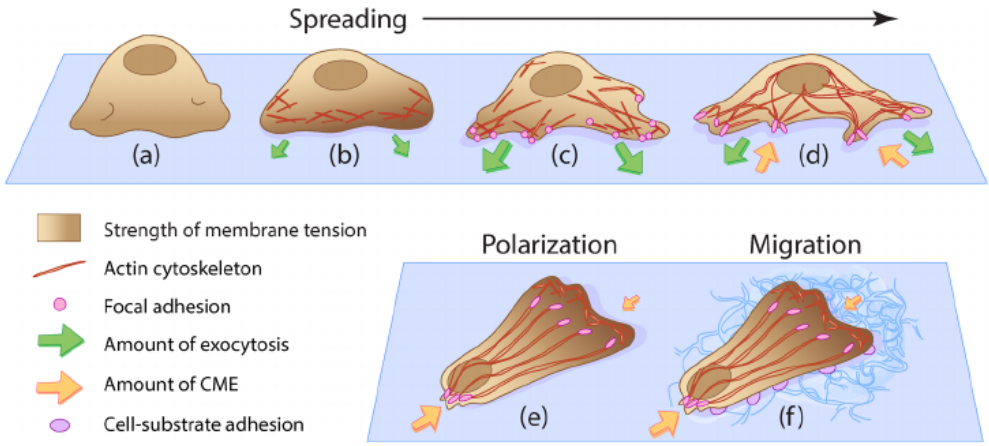

migrating cells, as clathrin-coated structures form more easily at the trailing edge than the leading edge, which is quantified by an increase in initiation and dissolution densities along with shortening of average lifetimes of clathrin coats at the trailing edge [Kural et al., 2015, Willy et al., 2017, Samaniego et al., 2007] (Figures 1H and 7A–7E). Similarly, with *in vivo* migration models such as *Drosophila* embryonic hemocytes, endocytic clathrin coats were found to be the least populated at lamellipodial protrusions of cells during their migration along the ventral nerve cord of the embryo [Willy et al., 2017] (Figures 7F–7J). Therefore, decreased CME dynamics upon increased membrane tension at the leading edge of migrating cells have been observed both *in vitro* and *in vivo*. Additional work of both approaches is needed to corroborate the role of membrane tension on regulating the spatial asymmetry of membrane trafficking pathways during cell migration.

Lastly, cell adhesion works in sync with actin dynamics and membrane trafficking to improve polarisation during cell migration. Adhesion complexes positioned in between cell–substrate and cell–cell contacts facilitate cell motility by their dynamic disassembly and assembly, where the latter takes place in protrusions. Adhesion components are endocytosed after disassembly and recycled to the plasma membrane for assembly of new adhesion sites [Ezratty et al., 2009, Ramírez-Santiago et al., 2016]. They also hold together actin cytoskeletal contacts with the membrane to modulate tension gradients induced by the contracting cytoskeleton [Hetmanski et al., 2019] (Figure 8F). Adhesion complexes have been well characterised to guide cell migration through various 2D and 3D environments [Batchelder and Yarar, 2010, Conway and Jacquemet, 2019] including formation of tubular clathrin/AP2 lattice structures (TCALs) to assist cells to form long protrusions and endure high tension arising

from migrating in stiff 3D environments [Elkhatib et al., 2017]. Importantly, it has been shown that clathrin itself is dispensable for TCAL attachment to substrate, demonstrating that TCAL formation is completely independent from clathrin's endocytic functions, yet both processes are required to promote effective cell migration [Elkhatib et al., 2017, Wessels et al., 2000]. Depending on the adhesive strength between the cell and the substrate, switching between 2D and 3D migration modes [Conway and Jacquemet, 2019] is necessary for cells to migrate with high persistence and polarity towards stiff substrate in complex environments [Hetmanski et al., 2019], but at the cost of decreased CME dynamics due to the formation of tight adhesions to the substrate [Batchelder and Yarar, 2010].

Adhesions between a cell and its substrate are essential for single cell directed migration but are involved in a more complex picture with the incorporation of more than one migrating cell. Cells during embryonic development, wound healing and metastasis [Vishwakarma et al., 2018] migrate heterogeneously and in effect encourage the formation of clear leader and follower cells within the migrating group [Vishwakarma et al., 2018, Rausch et al., 2013, Wang et al., 2016]. The formation of leader cells depends on the mechanical interaction of adhesion proteins with the actin cytoskeleton at cell–cell contacts [Vishwakarma et al., 2018, Peglion et al., 2014], while simultaneously receiving a mechanical push by follower cells [Vishwakarma et al., 2018]. These characteristics, along with physical curvature induced by the environment surrounding the migrating cells, instigate preferential choosing of a leader cell and thus promotes collective polarisation [Rausch et al., 2013]. Few studies on probing CME dynamics under tension gradients during collective cell migration exist due to its difficulty to image and lack of tools for non-invasive tension measurement [Gauthier et al., 2012]. This is additionally challenging due to the variety of factors that influence collective migration *in vivo* including, but not limited to chemical cues provided by growth factors, chemokines and cytokines [Doyle and Yamada, 2016], signalling between and within cells, and signalling between the cell and the environment [Wang et al., 2016, Ramel et al., 2013]. Altogether, a more detailed and systematic approach to understanding the role of CME under tension gradients in collective cell migration is required and perhaps possible with the advent of recent fluorescence microscopy approaches incorporating adaptive optics correction to minimise aberrations in deep tissue imaging [Liu et al., 2018].

Outlook

Metazoan cells are exposed to a myriad of mechanical forces within the 3D microenvironment they reside in [Dufort et al., 2011]. Mechanical cues generated during tissue morphogenesis regulate central developmental processes, such as, cytoskeleton remodelling, tissue differentiation and cell proliferation, through activation of mechanotransduction pathways. For example, in early-stage *Drosophila* embryos, artificially increasing the mechanical tension by gentle deformation of the ventral mesoderm can alter the developmental fate by blocking the endocytosis of receptors that regulate actomyosin organisation [Pouille et al., 2009]. Here, we reviewed some of the literature aimed for delineating the dynamic interplay between membrane mechanics and endocytic dynamics. The great majority of these attempts are based on *in vitro* studies conducted on isolated cells. However, we believe that newly developed approaches on the experimental and analytical fronts will allow researchers to conduct similar experiments *in situ*, that is, during physiological processes within intact tissues or multicellular organisms.

Tension in tissues relates to morphological changes during development, as well as fibroblastic transdifferentiations that lead to cardiovascular disorders and cancer metastasis [Dufort et al., 2011, Liu et al., 2007, Roy et al., 2000, Kaden et al., 2005, Edep et al., 2000, Pho et al., 2008, Calvo et al., 2013, Lu et al., 2012, Bergert et al., 2020]. Misregulation of physical cues, that is, abnormalities in the way cells respond to extracellular mechanical forces, can lead to a variety of pathologies such as cancer, cardiovascular diseases and developmental disorders [Jaalouk and Lammerding, 2009, Farge, 2011]. However, studies aimed for elucidating the mechanical states of cells are limited by the paucity of non-invasive probes applicable to systems in which cells are inaccessible [Gauthier et al., 2012]. During cellular processes, variation in CME dynamics reflects spatiotemporal gradients in tension throughout the cell membrane. The principle of membrane invagination during CME is similar to membrane tether

formation, which is used to quantify the apparent local membrane tension [Sheetz, 2001]. Therefore, spatiotemporal regulation of clathrin coat formation can potentially be utilised as an alternative tool for quantifying spatiotemporal variations in effective membrane tension within cellular contexts [Willy et al., 2017]. Furthermore, real-time monitoring and quantification of CME dynamics by growth rate distributions [Ferguson et al., 2016] could be transformed into imaging-based, noninvasive methodologies for generating maps of tension gradients within multicellular organisms during physiological processes.

Acknowledgements

C.K. is supported by NSF Faculty Early Career Development Program (Award number: 1751113) and NIH R01GM127526. U.D. is supported by the Pelotonia Fellowship Program. E. C. is supported by the Ohio State University Molecular Biophysics Training Program (NIH T32 GM118291-04). Any opinions, findings and conclusions expressed in this material are those of the author(s) and do not necessarily reflect those of the Pelotonia Fellowship Program or The Ohio State University.

Conflict of interest statement

The authors have declared no conflict of interest.

References

Aghamohammadzadeh, S. and Ayscough, K.R. (2009) Differential requirements for actin during yeast and mammalian endocytosis. Nat. Cell Biol. **11**, 1039–1042.

Agrawal, A. and Steigmann, D.J. (2009) Modeling protein-mediated morphology in biomembranes. Biomech. Model. Mechanobiol. **8**, 371–379.

Agrawal, N.J., Nukpezah, J. and Radhakrishnan, R. (2010) Minimal Mesoscale Model for Protein-Mediated Vesiculation in Clathrin-Dependent Endocytosis. PLoS Comput. Biol. **6**, e1000926.

Aguet, F., Antonescu, C.N., Mettlen, M., Schmid, S.L. and Danuser, G. (2013) Advances in Analysis of Low Signal-to-Noise Images Link Dynamin and AP2 to the Functions of an Endocytic Checkpoint. Dev. Cell **26**, 279–291.

Aguet, F., Upadhyayula, S., Gaudin, R., Chou, Y., Cocucci, E., He, K., Chen, B.-C., Mosaliganti, K., Pasham, M., Skillern, W., Legant, W.R., Liu, T.-L., Findlay, G., Marino, E., Danuser, G., Megason, S., Betzig, E. and Kirchhausen, T. (2016) Membrane dynamics of dividing cells imaged by lattice light-sheet microscopy. Mol. Biol. Cell **27**, 3418–3435.

Akisaka, T. and Yoshida, A. (2021) Surface distribution of heterogenous clathrin assemblies in resorbing osteoclasts. Exp. Cell Res. **399**, 112433.

Almeida-Souza, L., Frank, R.A.W., García-Nafría, J., Colussi, A., Gunawardana, N., Johnson, C.M., Yu, M., Howard, G., Andrews, B., Vallis, Y. and McMahon, H.T. (2018) A Flat BAR Protein Promotes Actin Polymerization at the Base of Clathrin-Coated Pits. Cell **174**, 325–337.e14.

Antonny, B. (2011) Mechanisms of Membrane Curvature Sensing. Annu. Rev. Biochem. **80**, 101–123.

Apodaca, G. (2002) Modulation of membrane traffic by mechanical stimuli. Am. J. Physiol. Ren. Physiol. **282**, F179–F190.

Avinoam, O., Schorb, M., Beese, C.J., Briggs, J.A.G. and Kaksonen, M. (2015) Endocytic sites mature by continuous bending and remodeling of the clathrin coat. Science **348**, 1369–1372.

Baschieri, F., Porshneva, K. and Montagnac, G. (2020) Frustrated clathrin-mediated endocytosis – causes and possible functions. J. Cell Sci. **133**, jcs240861.

Baschieri, F., Dayot, S., Elkhatib, N., Ly, N., Capmany, A., Schauer, K., Betz, T., Vignjevic, D.M., Poincloux, R. and Montagnac, G. (2018) Frustrated endocytosis controls contractility-independent mechanotransduction at clathrin-coated structures. Nat. Commun. **9**.

Batchelder, E.L., Hollopeter, G., Campillo, C., Mezanges, X., Jorgensen, E.M., Nassoy, P., Sens, P. and Plastino, J. (2011) Membrane tension regulates motility by controlling lamellipodium organization. Proc. Natl. Acad. Sci. **108**, 11429–11434.

Batchelder, E.M. and Yarar, D. (2010) Differential Requirements for Clathrin-dependent Endocytosis at Sites of Cell–Substrate Adhesion. Mol. Biol. Cell **21**, 3070–3079.

Bellve, K.D., Leonard, D., Standley, C., Lifshitz, L.M., Tuft, R.A., Hayakawa, A., Corvera, S. and Fogarty, K.E. (2006) Plasma Membrane Domains Specialized for Clathrin-mediated Endocytosis in Primary Cells. J. Biol. Chem. **281**, 16139–16146.

Benson, A.A. (1966) On the orientation of lipids in chloroplast and cell membranes. J. Am. Oil Chem. Soc. **43**, 265–270.

Bergert, M., Lembo, S., Sharma, S., Russo, L., Milovanović, D., Gretarsson, K.H., Börmel, M., Neveu, P.A., Hackett, J.A., Petsalaki, E. and Diz-Muñoz, A. (2021) Cell Surface Mechanics Gate Embryonic Stem Cell Differentiation. Cell Stem Cell **28**, 209–216.e4.

Betz, T., Lenz, M., Joanny, J.-F. and Sykes, C. (2009) ATP-dependent mechanics of red blood cells. Proc. Natl. Acad. Sci. **106**, 15320–15325.

Betz, T. and Sykes, C. (2012) Time resolved membrane fluctuation spectroscopy. Soft Matter **8**, 5317–5326.

Bianchini, P., Peres, C., Oneto, M., Galiani, S., Vicidomini, G. and Diaspro, A. (2015) STED nanoscopy: a glimpse into the future. Cell Tissue Res. **360**, 143–150.

Biancospino, M., Buel, G.R., Niño, C.A., Maspero, E., Scotto di Perrotolo, R., Raimondi, A., Redlingshöfer, L., Weber, J., Brodsky, F.M., Walters, K.J. and Polo, S. (2019) Clathrin light chain A drives selective myosin VI recruitment to clathrin-coated pits under membrane tension. Nat. Commun. **10.**

Bitoun, M., Maugenre, S., Jeannet, P.-Y., Lacène, E., Ferrer, X., Laforêt, P., Martin, J.-J., Laporte, J., Lochmüller, H., Beggs, A. H, Fardeau, M., Eymard, B., Romero, N. B and Guicheney, P. (2005) Mutations in dynamin 2 cause dominant centronuclear myopathy. Nat. Genet. **37**, 1207–1209.

Bitsikas, V., Corrêa, I.R. and Nichols, B.J. (2014) Clathrin-independent pathways do not contribute significantly to endocytic flux. eLife **3 .**

Bonneton, C., Sibarita, J.-B. and Thiery, J.-P. (1999) Relationship between cell migration and cell cycle during the initiation of epithelial to fibroblastoid transition. Cell Motil. Cytoskeleton **43**, 288–295.

Borner, G.H.H., Antrobus, R., Hirst, J., Bhumbra, G.S., Kozik, P., Jackson, L.P., Sahlender, D.A. and Robinson, M.S. (2012) Multivariate proteomic profiling identifies novel accessory proteins of coated vesicles. J. Cell Biol. **197**, 141–160.

Boucrot, E. and Kirchhausen, T. (2007) Endosomal recycling controls plasma membrane area during mitosis. Proc. Natl. Acad. Sci. **104**, 7939–7944.
Boulant, S., Kural, C., Zeeh, J.-C., Ubelmann, F. and Kirchhausen, T. (2011) Actin dynamics counteract membrane tension during clathrin-mediated endocytosis. Nat. Cell Biol. **13**, 1124–1131.
Bretscher, M.S. (1973) Membrane Structure: Some General Principles. Science **181**, 622–629.
Bretscher, M.S. (2008) Exocytosis provides the membrane for protrusion, at least in migrating fibroblasts. Nat. Rev. Mol. Cell Biol. **9**, 916–916.
Brod, J., Hellwig, A. and Wieland, F.T. (2020) Epsin but not AP-2 supports reconstitution of endocytic clathrin-coated vesicles. FEBS Lett. **594**, 2227–2239.
Bucher, D., Frey, F., Sochacki, K.A., Kummer, S., Bergeest, J.-P., Godinez, W.J., Kräusslich, H.-G., Rohr, K., Taraska, J.W., Schwarz, U.S. and Boulant, S. (2018) Clathrin-adaptor ratio and membrane tension regulate the flat-to-curved transition of the clathrin coat during endocytosis. Nat. Commun. **9.**
Busch, D.J., Houser, J.R., Hayden, C.C., Sherman, M.B., Lafer, E.M. and Stachowiak, J.C. (2015) Intrinsically disordered proteins drive membrane curvature. Nat. Commun. **6.**
Calvo, F., Ege, N., Grande-Garcia, A., Hooper, S., Jenkins, R.P., Chaudhry, S.I., Harrington, K., Williamson, P., Moeendarbary, E., Charras, G. and Sahai, E. (2013) Mechanotransduction and YAP-dependent matrix remodelling is required for the generation and maintenance of cancer-associated fibroblasts. Nat. Cell Biol. **15**, 637–646.
Canham, P.B. (1970) The minimum energy of bending as a possible explanation of the biconcave shape of the human red blood cell. J. Theor. Biol. **26**, 61–81.
Chapman, D. (1975) Phase transitions and fluidity characteristics of lipids and cell membranes. Q. Rev. Biophys. **8**, 185–235.
Chen, B.-C., Legant, W.R., Wang, K., Shao, L., Milkie, D.E., Davidson, M.W., Janetopoulos, C., Wu, X.S., Hammer, J.A., Liu, Z., English, B.P., Mimori-Kiyosue, Y., Romero, D.P., Ritter, A.T., Lippincott-Schwartz, J., Fritz-Laylin, L., Mullins, R.D., Mitchell, D.M., Bembenek, J.N., Reymann, A.-C., Böhme, R., Grill, S.W., Wang, J.T., Seydoux, G., Tulu, U.S., Kiehart, D.P. and Betzig, E. (2014) Lattice light-sheet microscopy: Imaging molecules to embryos at high spatiotemporal resolution. Science **346**, 1257998.
Chen, H., Ko, G., Zatti, A., Di Giacomo, G., Liu, L., Raiteri, E., Perucco, E., Collesi, C., Min, W., Zeiss, C., De Camilli, P. and Cremona, O. (2009) Embryonic arrest at midgestation and disruption of Notch signaling produced by the absence of both epsin 1 and epsin 2 in mice. Proc. Natl. Acad. Sci. **106**, 13838–13843.
Chen, Y., Yong, J., Martínez-Sánchez, A., Yang, Y., Wu, Y., De Camilli, P., Fernández-Busnadiego, R. and Wu, M. (2019) Dynamic instability of clathrin assembly provides proofreading control for endocytosis. J. Cell Biol. **218**, 3200–3211.
Chester, A.H. and Taylor, P.M. (2007) Molecular and functional characteristics of heart-valve interstitial cells. Philos. Trans. R. Soc. Lond. B Biol. Sci. **362**, 1437–1443.
Cocucci, E., Aguet, F., Boulant, S. and Kirchhausen, T. (2012) The First Five Seconds in the Life of a Clathrin-Coated Pit. Cell **150**, 495–507.
Cohen, A.E. and Shi, Z. (2020) Do Cell Membranes Flow Like Honey or Jiggle Like Jello?. BioEssays **42**, 1900142.
Colom, A., Derivery, E., Soleimanpour, S., Tomba, C., Molin, M.D., Sakai, N., González-Gaitán, M., Matile, S. and Roux, A. (2018) A fluorescent membrane tension probe. Nat. Chem. **10**, 1118–1125.
Conner, S.D. and Schmid, S.L. (2003) Regulated portals of entry into the cell. Nature **422**, 37–44.
Conway, J.R.W. and Jacquemet, G. (2019) Cell matrix adhesion in cell migration. Essays Biochem. **63**, 535–551.
Cunningham, C.C. (1995) Actin polymerization and intracellular solvent flow in cell surface blebbing. J. Cell Biol. **129**, 1589–1599.
Cureton, D.K., Massol, R.H., Whelan, S.P.J. and Kirchhausen, T. (2010) The Length of Vesicular Stomatitis Virus Particles Dictates a Need for Actin Assembly during Clathrin-Dependent Endocytosis. PLoS Pathog. **6**, e1001127.
Dai, J. and Sheetz, M.P. (1995) Mechanical properties of neuronal growth cone membranes studied by tether formation with laser optical tweezers. Biophys. J. **68**, 988–996.
Dai, J. and Sheetz, M.P. (1995) Regulation of Endocytosis, Exocytosis, and Shape by Membrane Tension. Cold Spring Harb. Symp. Quant. Biol. **60**, 567–571.
Dai, J. and Sheetz, M.P. (1999) Membrane Tether Formation from Blebbing Cells. Biophys. J. **77**, 3363–3370.
Dai, J., Ting-Beall, H.P. and Sheetz, M.P. (1997) The Secretion-coupled Endocytosis Correlates with Membrane Tension Changes in RBL 2H3 Cells. J. Gen. Physiol. **110**, 1–10.
Dalgliesh, G.L., Furge, K., Greenman, C., Chen, L., Bignell, G., Butler, A., Davies, H., Edkins, S., Hardy, C., Latimer, C., Teague, J., Andrews, J., Barthorpe, S., Beare, D., Buck, G., Campbell, P.J., Forbes, S., Jia, M., Jones, D., Knott, H., Kok, C.Y., Lau, K.W., Leroy, C., Lin, M.-L., McBride, D.J., Maddison, M., Maguire, S., McLay, K., Menzies, A., Mironenko, T., Mulderrig, L., Mudie, L., O'Meara, S., Pleasance, E., Rajasingham, A., Shepherd, R., Smith, R., Stebbings, L., Stephens, P., Tang, G., Tarpey, P.S., Turrell, K., Dykema, K.J., Khoo, S.K., Petillo, D., Wondergem, B., Anema, J., Kahnoski, R.J., Teh, B.T., Stratton, M.R. and Futreal, P.A. (2010) Systematic sequencing of renal carcinoma reveals inactivation of histone modifying genes. Nature **463**, 360–363.
Dambournet, D., Sochacki, K.A., Cheng, A.T., Akamatsu, M., Taraska, J.W., Hockemeyer, D. and Drubin, D.G. (2018) Genome-edited human stem cells expressing fluorescently labeled endocytic markers allow quantitative analysis of clathrin-mediated endocytosis during differentiation. J. Cell Biol. **217**, 3301–3311.
Danielli, J.F. and Davson, H. (1935) A contribution to the theory of permeability of thin films. J. Cell. Comp. Physiol. **5**, 495–508.
Dannhauser, P.N. and Ungewickell, E.J. (2012) Reconstitution of clathrin-coated bud and vesicle formation with minimal components. Nat. Cell Biol. **14**, 634–639.
den Otter, W.K. and Briels, W.J. (2011) The Generation of Curved Clathrin Coats from Flat Plaques. Traffic **12**, 1407–1416.
Derry, J.M.J., Ochs, H.D. and Francke, U. (1994) Isolation of a novel gene mutated in Wiskott-Aldrich syndrome. Cell **78**, 635–644.
Derry, J.M.J., Ochs, H.D. and Francke, U. (1994) Isolation of a novel gene mutated in Wiskott-Aldrich syndrome. Cell **79**, 635–644.
Diz-Muñoz, A., Fletcher, D.A. and Weiner, O.D. (2013) Use the force: membrane tension as an organizer of cell shape and motility. Trends Cell Biol. **23**, 47–53.
Diz-Muñoz, A., Thurley, K., Chintamen, S., Altschuler, S.J., Wu, L.F., Fletcher, D.A. and Weiner, O.D. (2016) Membrane Tension Acts Through PLD2 and mTORC2 to Limit Actin Network Assembly During Neutrophil Migration. PLOS Biol. **14**, e1002474.
Doherty, G.J. and McMahon, H.T. (2009) Mechanisms of Endocytosis. Annu. Rev. Biochem. **78**, 857–902.
Doyle, A.D. and Yamada, K.M. (2016) Mechanosensing via cell-matrix adhesions in 3D microenvironments. Exp. Cell Res. **343**, 60–66.
DuFort, C.C., Paszek, M.J. and Weaver, V.M. (2011) Balancing forces: architectural control of mechanotransduction. Nat. Rev. Mol. Cell Biol. **12**, 308–319.
Echarri, A. and Del Pozo, M.A. (2015) Caveolae - mechanosensitive membrane invaginations linked to actin filaments. J. Cell Sci. **128**, 2747–2758.
Edeling, M.A., Smith, C. and Owen, D. (2006) Life of a clathrin coat: insights from clathrin and AP structures. Nat. Rev. Mol. Cell Biol. **7**, 32–44.

Edep, M.E., Shirani, J., Wolf, P. and Brown, D.L. (2000) Matrix Metalloproteinase Expression in Nonrheumatic Aortic Stenosis. Cardiovasc. Pathol. **9**, 281–286.

Edidin, M. (2003) Lipids on the frontier: a century of cell-membrane bilayers. Nat. Rev. Mol. Cell Biol. **4**, 414–418.

Ehrlich, M., Boll, W., van Oijen, A., Hariharan, R., Chandran, K., Nibert, M.L. and Kirchhausen, T. (2004) Endocytosis by Random Initiation and Stabilization of Clathrin-Coated Pits. Cell **118**, 591–605.

Elkhatib, N., Bresteau, E., Baschieri, F., Rioja, A.L., van Niel, G., Vassilopoulos, S. and Montagnac, G. (2017) Tubular clathrin/AP-2 lattices pinch collagen fibers to support 3D cell migration. Science **356**, eaal4713.

Esmaeili Pourfarhangi, K., Cardenas De La Hoz, E., Cohen, A.R. and Gligorijevic, B. (2018) Contact guidance is cell cycle-dependent. APL Bioeng. **2**, 031904.

Evans, E. and Rawicz, W. (1990) Entropy-driven tension and bending elasticity in condensed-fluid membranes. Phys. Rev. Lett. **64**, 2094–2097.

Ezratty, E.J., Bertaux, C., Marcantonio, E.E. and Gundersen, G.G. (2009) Clathrin mediates integrin endocytosis for focal adhesion disassembly in migrating cells. J. Cell Biol. **187**, 733–747.

Farge, E. (2011) Chapter eight: Mechanotransduction in development. Curr. Top. Dev. Biol. **95**, 243–65.

Farsad, K. and Camilli, P.D. (2003) Mechanisms of membrane deformation. Curr. Opin. Cell Biol. **15**, 372–381.

Ferguson, J.P., Willy, N.M., Heidotting, S.P., Huber, S.D., Webber, M.J. and Kural, C. (2016) Deciphering dynamics of clathrin-mediated endocytosis in a living organism. J. Cell Biol. **214**, 347–358.

Ferguson, J.P., Huber, S.D., Willy, N.M., Aygün, E., Goker, S., Atabey, T. and Kural, C. (2017) Mechanoregulation of clathrin-mediated endocytosis. J. Cell Sci. **130**, 3631–3636.

Ferguson, S., Raimondi, A., Paradise, S., Shen, H., Mesaki, K., Ferguson, A., Destaing, O., Ko, G., Takasaki, J., Cremona, O., O' Toole, E. and De Camilli, P. (2009) Coordinated Actions of Actin and BAR Proteins Upstream of Dynamin at Endocytic Clathrin-Coated Pits. Dev. Cell **17**, 811–822.

Fielding, A.B. and Royle, S.J. (2013) Mitotic inhibition of clathrin-mediated endocytosis. Cell. Mol. Life Sci. **70**, 3423–3433.

Fiolka, R., Shao, L., Rego, E.H., Davidson, M.W. and Gustafsson, M.G.L. (2012) Time-lapse two-color 3D imaging of live cells with doubled resolution using structured illumination. Proc. Natl. Acad. Sci. **109**, 5311–5315.

Fogelson, B. and Mogilner, A. (2014) Computational Estimates of Membrane Flow and Tension Gradient in Motile Cells. PLoS ONE **9**, e84524.

Ford, M.G.J., Mills, I.G., Peter, B.J., Vallis, Y., Praefcke, G.J.K., Evans, P.R. and McMahon, H.T. (2002) Curvature of clathrin-coated pits driven by epsin. Nature **419**, 361–366.

Franck, A., Lainé, J., Moulay, G., Lemerle, E., Trichet, M., Gentil, C., Benkhelifa-Ziyyat, S., Lacène, E., Bui, M.T., Brochier, G., Guicheney, P., Romero, N., Bitoun, M. and Vassilopoulos, S. (2019) Clathrin plaques and associated actin anchor intermediate filaments in skeletal muscle. Mol. Biol. Cell **30**, 579–590.

Frick, M., Bright, N.A., Riento, K., Bray, A., Merrified, C. and Nichols, B.J. (2007) Coassembly of Flotillins Induces Formation of Membrane Microdomains, Membrane Curvature, and Vesicle Budding. Curr. Biol. **17**, 1151–1156.

Gérard, C. and Goldbeter, A. (2014) The balance between cell cycle arrest and cell proliferation: control by the extracellular matrix and by contact inhibition. Interface Focus **4**, 20130075.

Gögler, M., Betz, T. and Käs, J.A. (2007) Simultaneous manipulation and detection of living cell membrane dynamics. Optics Letters **32**, 1893.

Gabella, C., Bertseva, E., Bottier, C., Piacentini, N., Bornert, A., Jeney, S., Forró, L., Sbalzarini, I.F., Meister, J.-J. and Verkhovsky, A.B. (2014) Contact Angle at the Leading Edge Controls Cell Protrusion Rate. Curr. Biol. **24**, 1126–1132.

Gaidarov, I., Santini, F., Warren, R.A. and Keen, J.H. (1999) Spatial control of coated-pit dynamics in living cells. Nat. Cell Biol. **1**, 1–7.

Galletta, B.J., Mooren, O.L. and Cooper, J.A. (2010) Actin dynamics and endocytosis in yeast and mammals. Curr. Opin. Biotechnol. **21**, 604–610.

Gauthier, N.C., Fardin, M.A., Roca-Cusachs, P. and Sheetz, M.P. (2011) Temporary increase in plasma membrane tension coordinates the activation of exocytosis and contraction during cell spreading. Proc. Natl. Acad. Sci. **108**, 14467–14472.

Gauthier, N.C., Rossier, O.M., Mathur, A., Hone, J.C. and Sheetz, M.P. (2009) Plasma Membrane Area Increases with Spread Area by Exocytosis of a GPI-anchored Protein Compartment. Mol. Biol. Cell **20**, 3261–3272.

Gauthier, N.C., Masters, T.A. and Sheetz, M.P. (2012) Mechanical feedback between membrane tension and dynamics. Trends Cell Biol. **22**, 527–535.

Gauthier, N.C., Masters, T.A. and Sheetz, M.P. (2012) Mechanical feedback between membrane tension and dynamics. Trends Cell Biol. **22**, 527–535.

Giani, M., den Otter, W.K. and Briels, W.J. (2017) Early stages of clathrin aggregation at a membrane in coarse-grained simulations. J. Chem. Phys. **146**, 155102.

Giani, M., den Otter, W.K. and Briels, W.J. (2016) Clathrin Assembly Regulated by Adaptor Proteins in Coarse-Grained Models. Biophys. J. **111**, 222–235.

Gorter, E. and Grendel, F. (1925) ON BIMOLECULAR LAYERS OF LIPOIDS ON THE CHROMOCYTES OF THE BLOOD. J. Exp. Med. **41**, 439–443.

Grove, J., Metcalf, D.J., Knight, A.E., Wavre-Shapton, S.T., Sun, T., Protonotarios, E.D., Griffin, L.D., Lippincott-Schwartz, J. and Marsh, M. (2014) Flat clathrin lattices: stable features of the plasma membrane. Mol. Biol. Cell **25**, 3581–3594.

Guo, Y., Li, D., Zhang, S., Yang, Y., Liu, J.-J., Wang, X., Liu, C., Milkie, D.E., Moore, R.P., Tulu, U.S., Kiehart, D.P., Hu, J., Lippincott-Schwartz, J., Betzig, E. and Li, D. (2018) Visualizing Intracellular Organelle and Cytoskeletal Interactions at Nanoscale Resolution on Millisecond Timescales. Cell **175**, 1430–1442.e17.

Hansen, C.G., Bright, N.A., Howard, G. and Nichols, B.J. (2009) SDPR induces membrane curvature and functions in the formation of caveolae. Nat. Cell Biol. **11**, 807–814.

Happel, J. (1959) Viscous flow relative to arrays of cylinders. AIChE J. **5**, 174–177.

Harold, D., Abraham, R., Hollingworth, P., Sims, R., Gerrish, A., Hamshere, M.L., Pahwa, J.S., Moskvina, V., Dowzell, K., Williams, A., Jones, N., Thomas, C., Stretton, A., Morgan, A.R., Lovestone, S., Powell, J., Proitsi, P., Lupton, M.K., Brayne, C., Rubinsztein, D.C., Gill, M., Lawlor, B., Lynch, A., Morgan, K., Brown, K.S., Passmore, P.A., Craig, D., McGuinness, B., Todd, S., Holmes, C., Mann, D., Smith, A.D., Love, S., Kehoe, P.G., Hardy, J., Mead, S., Fox, N., Rossor, M., Collinge, J., Maier, W., Jessen, F., Schürmann, B., Heun, R., van den Bussche, H., Heuser, I., Kornhuber, J., Wiltfang, J., Dichgans, M., Frölich, L., Hampel, H., Hüll, M., Rujescu, D., Goate, A.M., Kauwe, J.S.K., Cruchaga, C., Nowotny, P., Morris, J.C., Mayo, K., Sleegers, K., Bettens, K., Engelborghs, S., De Deyn, P.P., Van Broeckhoven, C., Livingston, G., Bass, N.J., Gurling, H., McQuillin, A., Gwilliam, R., Deloukas, P., Al-Chalabi, A., Shaw, C.E., Tsolaki, M., Singleton, A.B., Guerreiro, R., Mühleisen, T.W., Nöthen, M.M., Moebus, S., Jöckel, K.-H., Klopp, N., Wichmann, H.-E., Carrasquillo, M.M., Pankratz, V.S., Younkin, S.G., Holmans, P.A., O'Donovan, M., Owen, M.J. and Williams, J. (2009) Genome-wide association study identifies variants at CLU

and PICALM associated with Alzheimer's disease. Nat. Genet. **41**, 1088–1093.
Harrison, S.C. and Kirchhausen, T. (1983) Clathrin, cages, and coated vesicles. Cell **33**, 650–652.
Hassinger, J.E., Oster, G., Drubin, D.G. and Rangamani, P. (2017) Design principles for robust vesiculation in clathrin-mediated endocytosis. Proc. Natl. Acad. Sci. **114**, E1118–E1127.
Haucke, V. and Kozlov, M.M. (2018) Membrane remodeling in clathrin-mediated endocytosis. J. Cell Sci. **131**, jcs216812.
Helfrich, W. (1973) Elastic Properties of Lipid Bilayers: Theory and Possible Experiments. Zeitschrift für Naturforschung C **28**, 693–703.
Heng, Y.-W. and Koh, C.-G. (2010) Actin cytoskeleton dynamics and the cell division cycle. Int. J. Biochem. Cell Biol. **42**, 1622–1633.
Henne, W.M., Boucrot, E., Meinecke, M., Evergren, E., Vallis, Y., Mittal, R. and McMahon, H.T. (2010) FCHo Proteins Are Nucleators of Clathrin-Mediated Endocytosis. Science **328**, 1281–1284.
Heuser, J.E., Keen, J.H., Amende, L.M., Lippoldt, R.E. and Prasad, K. (1987) Deep-etch visualization of 27S clathrin: a tetrahedral tetramer. J. Cell Biol. **105**, 1999–2009.
Heuser, J. (1980) Three-dimensional visualization of coated vesicle formation in fibroblasts. J. Cell Biol. **84**, 560–583.
Heuser, J. (1989) Effects of cytoplasmic acidification on clathrin lattice morphology. J. Cell Biol. **108**, 401–411.
Hochmuth, F.M., Shao, J.Y., Dai, J. and Sheetz, M.P. (1996) Deformation and flow of membrane into tethers extracted from neuronal growth cones. Biophys. J. **70**, 358–369.
Hochmuth, R.M. (2000) Micropipette aspiration of living cells. Journal of Biomechanics **33**, 15–22.
Hong, S.H., Cortesio, C.L. and Drubin, D.G. (2015) Machine-Learning-Based Analysis in Genome-Edited Cells Reveals the Efficiency of Clathrin-Mediated Endocytosis. Cell Rep. **12**, 2121–2130.
Houk, A.R., Jilkine, A., Mejean, C.O., Boltyanskiy, R., Dufresne, E.R., Angenent, S.B., Altschuler, S.J., Wu, L.F. and Weiner, O.D. (2012) Membrane Tension Maintains Cell Polarity by Confining Signals to the Leading Edge during Neutrophil Migration. Cell **148**, 175–188.
Huang, S., Chen, C.S. and Ingber, D.E. (1998) Control of Cyclin D1, p27Kip1, and Cell Cycle Progression in Human Capillary Endothelial Cells by Cell Shape and Cytoskeletal Tension. Mol. Biol. Cell **9**, 3179–3193.
Hyman, T., Shmuel, M. and Altschuler, Y. (2006) Actin Is Required for Endocytosis at the Apical Surface of Madin-Darby Canine Kidney Cells where ARF6 and Clathrin Regulate the Actin Cytoskeleton. Mol. Biol. Cell **17**, 427–437.
Irajizad, E., Walani, N., Veatch, S.L., Liu, A.P. and Agrawal, A. (2017) Clathrin polymerization exhibits high mechano-geometric sensitivity. Soft Matter **13**, 1455–1462.
Jaalouk, D.E. and Lammerding, J. (2009) Mechanotransduction gone awry. Nat. Rev. Mol. Cell Biol. **10**, 63–73.
Jacobson, K., Liu, P. and Lagerholm, B. Christoffer (2019) The Lateral Organization and Mobility of Plasma Membrane Components. Cell **177**, 806–819.
Jain, N., Moeller, J. and Vogel, V. (2019) Mechanobiology of Macrophages: How Physical Factors Coregulate Macrophage Plasticity and Phagocytosis. Annu. Rev. Biomed. Eng. **21**, 267–297.
Jaqaman, K., Loerke, D., Mettlen, M., Kuwata, H., Grinstein, S., Schmid, S.L. and Danuser, G. (2008) Robust single-particle tracking in live-cell time-lapse sequences. Nat. Methods **5**, 695–702.
Jarsch, I.K., Daste, F. and Gallop, J.L. (2016) Membrane curvature in cell biology: An integration of molecular mechanisms. J. Cell Biol. **214**, 375–387.
Jones, M.C., Askari, J.A., Humphries, J.D. and Humphries, M.J. (2018) Cell adhesion is regulated by CDK1 during the cell cycle. J. Cell Biol. **217**, 3203–3218.
Jones, S.A., Shim, S.-H., He, J. and Zhuang, X. (2011) Fast, three-dimensional super-resolution imaging of live cells. Nat. Methods **8**, 499–505.
Joseph, J.G., Osorio, C., Yee, V., Agrawal, A. and Liu, A.P. (2020) Complimentary action of structured and unstructured domains of epsin supports clathrin-mediated endocytosis at high tension. Commun. Biol. **3.**
Joseph, J.G. and Liu, A.P. (2020) Mechanical Regulation of Endocytosis: New Insights and Recent Advances. Adv. Biosyst. **4**, 1900278.
Kaden, J.J., Dempfle, C.-E., Grobholz, R., Fischer, C.S., Vocke, D.C., Kılıç, R., Sarıkoç, A., Piñol, R., Hagl, S., Lang, S., Brueckmann, M. and Borggrefe, M. (2005) Inflammatory regulation of extracellular matrix remodeling in calcific aortic valve stenosis. Cardiovasc. Pathol. **14**, 80–87.
Kadlecova, Z., Spielman, S.J., Loerke, D., Mohanakrishnan, A., Reed, D.K. and Schmid, S.L. (2017) Regulation of clathrin-mediated endocytosis by hierarchical allosteric activation of AP2. J. Cell Biol. **216**, 167–179.
Kan, Z., Jaiswal, B.S., Stinson, J., Janakiraman, V., Bhatt, D., Stern, H.M., Yue, P., Haverty, P.M., Bourgon, R., Zheng, J., Moorhead, M., Chaudhuri, S., Tomsho, L.P., Peters, B.A., Pujara, K., Cordes, S., Davis, D.P., Carlton, V.E.H., Yuan, W., Li, L., Wang, W., Eigenbrot, C., Kaminker, J.S., Eberhard, D.A., Waring, P., Schuster, S.C., Modrusan, Z., Zhang, Z., Stokoe, D., de Sauvage, F.J., Faham, M. and Seshagiri, S. (2010) Diverse somatic mutation patterns and pathway alterations in human cancers. Nature **466**, 869–873.
Kanaseki, T. and Kadota, K. (1969) THE "VESICLE IN A BASKET". J. Cell Biol. **42**, 202–220.
Kaur, S., Fielding, A.B., Gassner, G., Carter, N.J. and Royle, S.J. (2014) An unmet actin requirement explains the mitotic inhibition of clathrin-mediated endocytosis. eLife **3 .**
Keren, K. (2011) Cell motility: the integrating role of the plasma membrane. Eur. Biophys. J. **40**, 1013–1027.
Keren, K., Pincus, Z., Allen, G.M., Barnhart, E.L., Marriott, G., Mogilner, A. and Theriot, J.A. (2008) Mechanism of shape determination in motile cells. Nature **453**, 475–480.
Kirchhausen, T., Owen, D. and Harrison, S.C. (2014) Molecular Structure, Function, and Dynamics of Clathrin-Mediated Membrane Traffic. Cold Spring Harbor Perspect. Biol. **6**, a016725–a016725.
Kirchhausen, T. (2009) Imaging endocytic clathrin structures in living cells. Trends Cell Biol. **19**, 596–605.
Kirchhausen, T. (2012) Bending membranes. Nat. Cell Biol. **14**, 906–908.
Kirchhausen, T. (1993) Coated pits and coated vesicles — sorting it all out. Curr. Opin. Struct. Biol. **3**, 182–188.
Kirchhausen, T. (2000) Clathrin. Annu. Rev. Biochem. **69**, 699–727.
Kirchhausen, T. and Harrison, S.C. (1981) Protein organization in clathrin trimers. Cell **23**, 755–761.
Kozlov, M.M. and Mogilner, A. (2007) Model of Polarization and Bistability of Cell Fragments. Biophys. J. **93**, 3811–3819.
Kozlov, M.M., Campelo, F., Liska, N., Chernomordik, L.V., Marrink, S.J. and McMahon, H.T. (2014) Mechanisms shaping cell membranes. Curr. Opin. Cell Biol. **29** 53–60.
Krause, M., Yang, F.W., te Lindert, M., Isermann, P., Schepens, J., Maas, R.J.A., Venkataraman, C., Lammerding, J., Madzvamuse, A., Hendriks, W., te Riet, J. and Wolf, K. (2019) Cell migration through three-dimensional confining pores: speed accelerations by deformation and recoil of the nucleus. Philos. Trans. R. Soc. Lond. B Biol. Sci. **374**, 20180225.
Kural, C., Tacheva-Grigorova, S.K., Boulant, S., Cocucci, E., Baust, T., Duarte, D. and Kirchhausen, T. (2012) Dynamics of Intracellular Clathrin/AP1- and Clathrin/AP3-Containing Carriers. Cell Rep. **2**, 1111–1119.

Kural, C., Akatay, A.A., Gaudin, R., Chen, B.-C., Legant, W.R., Betzig, E. and Kirchhausen, T. (2015) Asymmetric formation of coated pits on dorsal and ventral surfaces at the leading edges of motile cells and on protrusions of immobile cells. Mol. Biol. Cell **26**, 2044–2053.

Kural, C. and Kirchhausen, T. (2012) Live-cell imaging of clathrin coats. Methods Enzymol.. **505**, 59–80.

Kusumi, A., Fujiwara, T.K., Chadda, R., Xie, M., Tsunoyama, T.A., Kalay, Z., Kasai, R.S. and Suzuki, K.G.N. (2012) Dynamic Organizing Principles of the Plasma Membrane that Regulate Signal Transduction: Commemorating the Fortieth Anniversary of Singer and Nicolson's Fluid-Mosaic Model. Annu. Rev. Cell Dev. Biol. **28**, 215–250.

Lafaurie-Janvore, J., Maiuri, P., Wang, I., Pinot, M., Manneville, J.-B., Betz, T., Balland, M. and Piel, M. (2013) ESCRT-III Assembly and Cytokinetic Abscission Are Induced by Tension Release in the Intercellular Bridge. Science **339**, 1625–1629.

Lampe, M., Vassilopoulos, S. and Merrifield, C. (2016) Clathrin coated pits, plaques and adhesion. J. Struct. Biol. **196**, 48–56.

Larson, R. G (1999). The Structure and Rheology of Complex Fluids, Oxford University Press Inc, New York.

Le Roux, A.-L., Quiroga, X., Walani, N., Arroyo, M. and Roca-Cusachs, P. (2019) The plasma membrane as a mechanochemical transducer. Philos. Trans. R. Soc. Lond. B Biol. Sci. **374**, 20180221.

Lee, L.M. and Liu, A.P. (2015) A microfluidic pipette array for mechanophenotyping of cancer cells and mechanical gating of mechanosensitive channels. Lab on a Chip **15**, 264–273.

LeGoff, L. and Lecuit, T. (2016) Mechanical Forces and Growth in Animal Tissues. Cold Spring Harbor Perspect. Biol. **8**, a019232.

Leyton-Puig, D., Isogai, T., Argenzio, E., van den Broek, B., Klarenbeek, J., Janssen, H., Jalink, K. and Innocenti, M. (2017) Flat clathrin lattices are dynamic actin-controlled hubs for clathrin-mediated endocytosis and signalling of specific receptors. Nat. Commun. **8.**

Li, D., Shao, L., Chen, B.-C., Zhang, X., Zhang, M., Moses, B., Milkie, D.E., Beach, J.R., Hammer, J.A., Pasham, M., Kirchhausen, T., Baird, M.A., Davidson, M.W., Xu, P. and Betzig, E. (2015) Extended-resolution structured illumination imaging of endocytic and cytoskeletal dynamics. Science **349**, aab3500–aab3500.

Lieber, A.D., Schweitzer, Y., Kozlov, M.M. and Keren, K. (2015) Front-to-Rear Membrane Tension Gradient in Rapidly Moving Cells. Biophys. J. **108**, 1599–1603.

Lieber, A.D., Yehudai-Resheff, S., Barnhart, E.L., Theriot, J.A. and Keren, K. (2013) Membrane Tension in Rapidly Moving Cells Is Determined by Cytoskeletal Forces. Curr. Biol. **23**, 1409–1417.

Liu, A.P., Loerke, D., Schmid, S.L. and Danuser, G. (2009) Global and Local Regulation of Clathrin-Coated Pit Dynamics Detected on Patterned Substrates. Biophys. J. **97**, 1038–1047.

Liu, A.C., Joag, V.R. and Gotlieb, A.I. (2007) The Emerging Role of Valve Interstitial Cell Phenotypes in Regulating Heart Valve Pathobiology. Am. J. Pathol. **171**, 1407–1418.

Liu, J., Du, J. and Wang, Y. (2019) CDK5 inhibits the clathrin-dependent internalization of TRPV1 by phosphorylating the clathrin adaptor protein AP2μ2. Sci. Signal. **12**, eaaw2040.

Liu, L.R., Hood, J.D., Yu, Y., Zhang, J.T., Hutzler, N.R., Rosenband, T. and Ni, K.-K. (2018) Building one molecule from a reservoir of two atoms. Science **360**, 900–903.

Liu, L., Shi, H., Chen, X. and Wang, Z. (2011) Regulation of EGF-Stimulated EGF Receptor Endocytosis During M Phase. Traffic **12**, 201–217.

Lock, J.G., Jones, M.C., Askari, J.A., Gong, X., Oddone, A., Olofsson, H., Göransson, S., Lakadamyali, M., Humphries, M.J. and Strömblad, S. (2018) Reticular adhesions are a distinct class of cell-matrix adhesions that mediate attachment during mitosis. Nat. Cell Biol., **20**, 1290–1302.

Loerke, D., Mettlen, M., Yarar, D., Jaqaman, K., Jaqaman, H., Danuser, G. and Schmid, S.L. (2009) Cargo and Dynamin Regulate Clathrin-Coated Pit Maturation. PLOS Biol. **7**, e1000057.

Loerke, D., Mettlen, M., Schmid, S.L. and Danuser, G. (2011) Measuring the Hierarchy of Molecular Events During Clathrin-Mediated Endocytosis. Traffic **12**, 815–825.

Loh, J., Chuang, M.-C., Lin, S.-S., Joseph, J., Su, Y.-A., Hsieh, T.-L., Chang, Y.-C., Liu, A.P. and Liu, Y.-W. (2019) An acute decrease in plasma membrane tension induces macropinocytosis via PLD2 activation. J. Cell Sci. **132**, jcs232579.

Lu, P., Weaver, V.M. and Werb, Z. (2012) The extracellular matrix: A dynamic niche in cancer progression. J. Cell Biol. **196**, 395–406.

Ma, X., Lynch, H.E., Scully, P.C. and Hutson, M.S. (2009) Probing embryonic tissue mechanics with laser hole drilling. Phys. Biol. **6**, 036004.

Macosko, C.W. (1994). Rheology principles measurements and applications, Willey -VCH, New York,.

Mahmood, Md. I., Noguchi, H. and Okazaki, K.-i. (2019) Curvature induction and sensing of the F-BAR protein Pacsin1 on lipid membranes via molecular dynamics simulations. Sci. Rep. **9.**

Majoul, I., Schmidt, T., Pamasanova, M., Boutkevich, E., Kozlov, Y. and Söling, H. (2002) Differential expression of receptors for Shiga and Cholera toxin is regulated by the cell cycle. J. Cell Sci. **115**, 817–826.

Margadant, C., Cremers, L., Sonnenberg, A. and Boonstra, J. (2013) MAPK uncouples cell cycle progression from cell spreading and cytoskeletal organization in cycling cells. Cell. Mol. Life Sci. **70**, 293–307.

Mashl, R.J. and Bruinsma, R.F. (1998) Spontaneous-Curvature Theory of Clathrin-Coated Membranes. Biophys. J. **74**, 2862–2875.

Massol, R.H., Boll, W., Griffin, A.M. and Kirchhausen, T. (2006) A burst of auxilin recruitment determines the onset of clathrin-coated vesicle uncoating. Proc. Natl. Acad. Sci. **103**, 10265–10270.

Masters, T.A., Pontes, B., Viasnoff, V., Li, Y. and Gauthier, N.C. (2013) Plasma membrane tension orchestrates membrane trafficking, cytoskeletal remodeling, and biochemical signaling during phagocytosis. Proc. Natl. Acad. Sci. **110**, 11875–11880.

Maupin, P and Pollard, T D (1983) Improved preservation and staining of HeLa cell actin filaments, clathrin-coated membranes, and other cytoplasmic structures by tannic acid-glutaraldehyde-saponin fixation. J. Cell Biol. **96**, 51–62.

McMahon, H.T. and Boucrot, E. (2015) Membrane curvature at a glance. J. Cell Sci. **128**, 1065–1070.

McMahon, H.T. and Boucrot, E. (2011) Molecular mechanism and physiological functions of clathrin-mediated endocytosis. Nat. Rev. Mol. Cell Biol. **12**, 517–533.

McMahon, H.T. and Gallop, J.L. (2005) Membrane curvature and mechanisms of dynamic cell membrane remodelling. Nature **438**, 590–596.

Meinecke, M., Boucrot, E., Camdere, G., Hon, W.-C., Mittal, R. and McMahon, H.T. (2013) Cooperative Recruitment of Dynamin and BIN/Amphiphysin/Rvs (BAR) Domain-containing Proteins Leads to GTP-dependent Membrane Scission*. J. Biol. Chem. **288**, 6651–6661.

Merrifield, C.J., Feldman, M.E., Wan, L. and Almers, W. (2002) Imaging actin and dynamin recruitment during invagination of single clathrin-coated pits. Nat. Cell Biol. **4**, 691–698.

Mettlen, M. and Danuser, G. (2014) Imaging and Modeling the Dynamics of Clathrin-Mediated Endocytosis. Cold Spring Harbor Perspect. Biol. **6**, a017038–a017038.

Meyerholz, A., Hinrichsen, L., Groos, S., Esk, P.-C., Brandes, G. and Ungewickell, E.J. (2005) Effect of Clathrin Assembly Lymphoid Myeloid Leukemia Protein Depletion on Clathrin Coat Formation. Traffic **6**, 1225–1234.

Miki, H., Suetsugu, S. and Takenawa, T. (1998) WAVE, a novel WASP-family protein involved in actin reorganization induced by Rac. EMBO J. **17**, 6932–6941.
Miller, S.E., Mathiasen, S., Bright, N.A., Pierre, F., Kelly, B.T., Kladt, N., Schauss, A., Merrifield, C.J., Stamou, D., Höning, S. and Owen, D.J. (2015) CALM Regulates Clathrin-Coated Vesicle Size and Maturation by Directly Sensing and Driving Membrane Curvature. Dev. Cell **33**, 163–175.
Mishra, S.K., Watkins, S.C. and Traub, L.M. (2002) The autosomal recessive hypercholesterolemia (ARH) protein interfaces directly with the clathrin-coat machinery. Proc. Natl. Acad. Sci. **99**, 16099–16104.
Mitchison, T.J. and Cramer, L.P. (1996) Actin-Based Cell Motility and Cell Locomotion. Cell **84**, 371–379.
Mitsunari, T., Nakatsu, F., Shioda, N., Love, P.E., Grinberg, A., Bonifacino, J.S. and Ohno, H. (2005) Clathrin Adaptor AP-2 Is Essential for Early Embryonal Development. Mol. Cell. Biol. **25**, 9318–9323.
Monier, S., Parton, R.G., Vogel, F., Behlke, J., Henske, A. and Kurzchalia, T.V. (1995) VIP21-caveolin, a membrane protein constituent of the caveolar coat, oligomerizes in vivo and in vitro. Mol. Biol. Cell **6**, 911–927.
Moulay, G., Lainé, J., Lemaître, M., Nakamori, M., Nishino, I., Caillol, G., Mamchaoui, K., Julien, L., Dingli, F., Loew, D., Bitoun, M., Leterrier, C., Furling, D. and Vassilopoulos, Stéphane (2020) Alternative splicing of clathrin heavy chain contributes to the switch from coated pits to plaques. J. Cell Biol. **219.**
Musacchio, A., Smith, C.J., Roseman, A.M., Harrison, S.C., Kirchhausen, T. and Pearse, B.M.F. (1999) Functional Organization of Clathrin in Coats. Mol. Cell **3**, 761–770.
Narasimhan, M., Johnson, A., Prizak, R. and Friml, J. (2019) Evolutionary unique mechanistic framework of clathrin-mediated endocytosis in plants. bioRxiv 1–30.
Ng, I.C., Pawijit, P., Tan, J. and Yu, H., in Encyclopedia of Biomedical Engineering, R. Narayan, Ed. (2019), pp. 225–236.
Nicolson, G.L. (2014) The Fluid—Mosaic Model of Membrane Structure: Still relevant to understanding the structure, function and dynamics of biological membranes after more than 40years. Biochim. Biophys. Acta (BBA) - Biomembranes **1838**, 1451–1466.
Oliver, J.M., Seagrave, J.C., Pfeiffer, J.R., Feibig, M.L. and Deanin, G.G. (1985) Surface functions during mitosis in rat basophilic leukemia cells. J. Cell Biol. **101**, 2156–2166.
Parsons, J.T., Horwitz, A.R. and Schwartz, M.A. (2010) Cell adhesion: integrating cytoskeletal dynamics and cellular tension. Nat. Rev. Mol. Cell Biol. **11**, 633–643.
Parton, R.G. and del Pozo, M.A. (2013) Caveolae as plasma membrane sensors, protectors and organizers. Nat. Rev. Mol. Cell Biol. **14**, 98–112.
Parton, R.G., Kozlov, M.M. and Ariotti, N. (2020) Caveolae and lipid sorting: Shaping the cellular response to stress. J. Cell Biol. **219.**
Pascolutti, R., Algisi, V., Conte, A., Raimondi, A., Pasham, M., Upadhyayula, S., Gaudin, R., Maritzen, T., Barbieri, E., Caldieri, G., Tordonato, C., Confalonieri, S., Freddi, S., Malabarba, M.G., Maspero, E., Polo, S., Tacchetti, C., Haucke, V., Kirchhausen, T., Di Fiore, P.P. and Sigismund, S. (2019) Molecularly Distinct Clathrin-Coated Pits Differentially Impact EGFR Fate and Signaling. Cell Rep. **27**, 3049–3061.e6.
Pearse, B.M.F. (1975) Coated vesicles from pig brain: Purification and biochemical characterization. J. Mol. Biol. **97**, 93–98.
Peglion, F., Llense, F. and Etienne-Manneville, S. (2014) Adherens junction treadmilling during collective migration. Nat. Cell Biol. **16**, 639–651.
Peter, B.J. (2004) BAR Domains as Sensors of Membrane Curvature: The Amphiphysin BAR Structure. Science **303**, 495–499.
Peukes, J. and Betz, T. (2014) Direct Measurement of the Cortical Tension during the Growth of Membrane Blebs. Biophys. J. **107**, 1810–1820.
Pho, M., Lee, W., Watt, D.R., Laschinger, C., Simmons, C.A. and McCulloch, C.A. (2008) Cofilin is a marker of myofibroblast differentiation in cells from porcine aortic cardiac valves. Am. J. Physiol. Heart Circ. Physiol. **294**, H1767–H1778.
Pinot, M., Vanni, S., Pagnotta, S., Lacas-Gervais, S., Payet, L.-A., Ferreira, T., Gautier, R., Goud, B., Antonny, B. and Barelli, H. (2014) Polyunsaturated phospholipids facilitate membrane deformation and fission by endocytic proteins. Science **345**, 693–697.
Pontes, B., Monzo, P. and Gauthier, N.C. (2017) Membrane tension: A challenging but universal physical parameter in cell biology. Semin. Cell Dev. Biol. **71** 30–41.
Pouille, P.-A., Ahmadi, P., Brunet, A.-C. and Farge, E. (2009) Mechanical Signals Trigger Myosin II Redistribution and Mesoderm Invagination in Drosophila Embryos. Sci. Signal. **2**, ra16–ra16.
Purushothaman, L.K. and Ungermann, C. (2018) Cargo induces retromer-mediated membrane remodeling on membranes. Mol. Biol. Cell **29**, 2709–2719.
Pypaert, M., Mundy, D., Souter, E., Labbé, J.C. and Warren, G. (1991) Mitotic cytosol inhibits invagination of coated pits in broken mitotic cells. J. Cell Biol. **114**, 1159–1166.
Ramírez-Santiago, G., Robles-Valero, J., Morlino, G., Cruz-Adalia, A., Pérez-Martínez, M., Zaldivar, A., Torres-Torresano, M., Chichón, F.J., Sorrentino, A., Pereiro, E., Carrascosa, J.L., Megías, D., Sorzano, C.O.S., Sánchez-Madrid, F. and Veiga, E. (2016) Clathrin regulates lymphocyte migration by driving actin accumulation at the cellular leading edge. Eur. J. Immunol. **46**, 2376–2387.
Ramírez-Santiago, G., Robles-Valero, J., Morlino, G., Cruz-Adalia, A., Pérez-Martínez, M., Zaldivar, A., Torres-Torresano, M., Chichón, F.J., Sorrentino, A., Pereiro, E., Carrascosa, J.L., Megías, D., Sorzano, C.O.S., Sánchez-Madrid, F. and Veiga, E. (2016) Clathrin regulates lymphocyte migration by driving actin accumulation at the cellular leading edge. Eur. J. Immunol. **46**, 2376–2387.
Ramel, D., Wang, X., Laflamme, C., Montell, D.J. and Emery, G. (2013) Rab11 regulates cell–cell communication during collective cell movements. Nat. Cell Biol. **15**, 317–324.
Rangamani, P., Fardin, M.-A., Xiong, Y., Lipshtat, A., Rossier, O., Sheetz, M.P. and Iyengar, R. (2011) Signaling Network Triggers and Membrane Physical Properties Control the Actin Cytoskeleton-Driven Isotropic Phase of Cell Spreading. Biophys. J. **100**, 845–857.
Raucher, D. and Sheetz, M.P. (2000) Cell Spreading and Lamellipodial Extension Rate Is Regulated by Membrane Tension. J. Cell Biol. **148**, 127–136.
Raucher, D. and Sheetz, M.P. (1999) Membrane Expansion Increases Endocytosis Rate during Mitosis. J. Cell Biol. **144**, 497–506.
Rausch, S., Das, T., Soiné, J.R.D., Hofmann, T.W., Boehm, C.H.J., Schwarz, U.S., Boehm, H. and Spatz, J.P. (2013) Polarizing cytoskeletal tension to induce leader cell formation during collective cell migration. Biointerphases **8**, 32.
Rawicz, W., Olbrich, K.C., McIntosh, T., Needham, D. and Evans, E. (2000) Effect of Chain Length and Unsaturation on Elasticity of Lipid Bilayers. Biophys. J. **79**, 328–339.
Reinhart-King, C.A., Dembo, M. and Hammer, D.A. (2005) The Dynamics and Mechanics of Endothelial Cell Spreading. Biophys. J. **89**, 676–689.
Riggi, M., Bourgoint, C., Macchione, M., Matile, S., Loewith, R. and Roux, A. (2019) TORC2 controls endocytosis through plasma membrane tension. J. Cell Biol. **218**, 2265–2276.
Riggi, M., Niewola-Staszkowska, K., Chiaruttini, N., Colom, A., Kusmider, B., Mercier, V., Soleimanpour, S., Stahl, M., Matile, S., Roux, A. and Loewith, R. (2018) Decrease in plasma membrane tension triggers PtdIns(4,5)P2 phase separation to inactivate TORC2. Nat. Cell Biol. **20**, 1043–1051.
Robinson, M.S. (2004) Adaptable adaptors for coated vesicles. Trends Cell Biol. **14**, 167–174.
Robinson, M.S. (2015) Forty Years of Clathrin-coated Vesicles. Traffic **16**, 1210–1238.

Rosselli-Murai, L.K., Yates, J.A., Yoshida, S., Bourg, J., Ho, K.K.Y., White, M., Prisby, J., Tan, X., Altemus, M., Bao, L., Wu, Z.-F., Veatch, S.L., Swanson, J.A., Merajver, S.D. and Liu, A.P. (2018) Loss of PTEN promotes formation of signaling-capable clathrin-coated pits. J. Cell Sci. **131**, jcs208926.

Saffarian, S., Cocucci, E. and Kirchhausen, T. (2009) Distinct Dynamics of Endocytic Clathrin-Coated Pits and Coated Plaques. PLOS Biol. **7**, e1000191.

Saffman, P.G. and Delbruck, M. (1975) Brownian motion in biological membranes. Proc. Natl. Acad. Sci. **72**, 3111–3113.

Sager, P.R., Brown, P.A. and Berlin, R.D. (1984) Analysis of transferrin recycling in mitotic and interphase hela cells by quantitative fluorescence microscopy. Cell **39**, 275–282.

Saias, L., Swoger, J., D'Angelo, A., Hayes, P., Colombelli, J., Sharpe, J., Salbreux, G. and Solon, J. (2015) Decrease in Cell Volume Generates Contractile Forces Driving Dorsal Closure. Dev. Cell **33**, 611–621.

Saleem, M., Morlot, S., Hohendahl, A., Manzi, J., Lenz, M. and Roux, A. (2015) A balance between membrane elasticity and polymerization energy sets the shape of spherical clathrin coats. Nat. Commun. **6.**

Samaniego, R., Sanchez-Martin, L., Estecha, A. and Sanchez-Mateos, P. (2007) Rho/ROCK and myosin II control the polarized distribution of endocytic clathrin structures at the uropod of moving T lymphocytes. J. Cell Sci. **120**, 3534–3543.

Schöneberg, J., Dambournet, D., Liu, T.-L., Forster, R., Hockemeyer, D., Betzig, E. and Drubin, D.G. (2018) 4D cell biology: big data image analytics and lattice light-sheet imaging reveal dynamics of clathrin-mediated endocytosis in stem cell–derived intestinal organoids. Mol. Biol. Cell **29**, 2959–2968.

Schmid, S.L. (1997) Clathrin-coated vesicle formation and protein sorting: An integrated process. Annu. Rev. Biochem. **66**, 511–548.

Seifert, U. (1997) Configurations of fluid membranes and vesicles. Adv. Phys. **46**, 13–137.

Sens, P. and Plastino, J. (2015) Membrane tension and cytoskeleton organization in cell motility. J. Phys. Condensed Matter **27**, 273103.

Sens, P. and Plastino, J. (2015) Membrane tension and cytoskeleton organization in cell motility. J. Phys. Condensed Matter **27**, 273103.

Sezgin, E., Levental, I., Mayor, S. and Eggeling, C. (2017) The mystery of membrane organization: composition, regulation and roles of lipid rafts. Nat. Rev. Mol. Cell Biol. **18**, 361–374.

Sheetz, M.P. (2001) Cell control by membrane–cytoskeleton adhesion. Nat. Rev. Mol. Cell Biol. **2**, 392–396.

Sheetz, M.P. and Dai, J. (1996) Modulation of membrane dynamics and cell motility by membrane tension. Trends Cell Biol. **6**, 85–89.

Sheetz, M.P., Sable, J.E. and Döbereiner, H.-G. (2006) Continuous membrane-cytoskeleton adhesion requires continuous accommodation to lipid and cytoskeleton dynamics. Annu. Rev. Biophys. Biomol. Struct. **35**, 417–434.

Shi, Z., Graber, Z.T., Baumgart, T., Stone, H.A. and Cohen, A.E. (2018) Cell Membranes Resist Flow. Cell **175**, 1769–1779.e13.

Shi, Z. and Baumgart, T. (2015) Membrane tension and peripheral protein density mediate membrane shape transitions. Nat. Commun. **6.**

Shraiman, B.I. (1997) On the Role of Assembly Kinetics in Determining the Structure of Clathrin Cages. Biophys. J. **72**, 953–957.

Simunovic, M., Voth, G.A., Callan-Jones, A. and Bassereau, P. (2015) When Physics Takes Over: BAR Proteins and Membrane Curvature. Trends Cell Biol. **25**, 780–792.

Singer, S.J. and Nicolson, G.L. (1972) The Fluid Mosaic Model of the Structure of Cell Membranes. Science **175**, 720–731.

Sinha, B., Köster, D., Ruez, R., Gonnord, P., Bastiani, M., Abankwa, D., Stan, R.V., Butler-Browne, G., Vedie, B., Johannes, L., Morone, N., Parton, R.G., Raposo, G., Sens, P., Lamaze, C. and Nassoy, P. (2011) Cells Respond to Mechanical Stress by Rapid Disassembly of Caveolae. Cell **144**, 402–413.

Smith, C.J. (1998) Clathrin coats at 21Aresolution: a cellular assembly designed to recycle multiple membrane receptors. EMBO J. **17**, 4943–4953.

Snijder, B., Sacher, R., Rämö, P., Damm, E.-M., Liberali, P. and Pelkmans, L. (2009) Population context determines cell-to-cell variability in endocytosis and virus infection. Nature **461**, 520–523.

Sochacki, K.A., Dickey, A.M., Strub, M.-P. and Taraska, J.W. (2017) Endocytic proteins are partitioned at the edge of the clathrin lattice in mammalian cells. Nat. Cell Biol. **19**, 352–361.

Sochacki, K.A. and Taraska, J.W. (2019) From Flat to Curved Clathrin: Controlling a Plastic Ratchet. Trends Cell Biol. **29**, 241–256.

Stachowiak, J.C., Schmid, E.M., Ryan, C.J., Ann, H.S., Sasaki, D.Y., Sherman, M.B., Geissler, P.L., Fletcher, D.A. and Hayden, C.C. (2012) Membrane bending by protein–protein crowding. Nat. Cell Biol. **14**, 944–949.

Stagg, S.M., Gürkan, C., Fowler, D.M., LaPointe, P., Foss, T.R., Potter, C.S., Carragher, B. and Balch, W.E. (2006) Structure of the Sec13/31 COPII coat cage. Nature **439**, 234–238.

Stanishneva-Konovalova, T.B., Derkacheva, N. I, Polevova, S.V. and Sokolova, O.S. (2016) The role of BAR domain proteins in the regulation of membrane dynamics. Acta Nat.. **8**, 60–69.

Staykova, M., Holmes, D.P., Read, C. and Stone, H.A. (2011) Mechanics of surface area regulation in cells examined with confined lipid membranes. Proc. Natl. Acad. Sci. **108**, 9084–9088.

Steinem, C. and Meinecke, M. (2021) ENTH domain-dependent membrane remodelling. Soft Matter **17**, 233–240.

Stewart, M.P., Toyoda, Y., Hyman, A.A. and Muller, D.J. (2011) Force probing cell shape changes to molecular resolution. Trends Biochem. Sci. **36**, 444–450.

Stoeckenius, W. and Engelman, D.M. (1969) Current models for the structure of biological membranes. J. Cell Biol. **42**, 613–646.

Sun, M., Graham, J.S., Hegedüs, B., Marga, F., Zhang, Y., Forgacs, G. and Grandbois, M. (2005) Multiple Membrane Tethers Probed by Atomic Force Microscopy. Biophys. J. **89**, 4320–4329.

Sweitzer, S.M. and Hinshaw, J.E. (1998) Dynamin Undergoes a GTP-Dependent Conformational Change Causing Vesiculation. Cell **93**, 1021–1029.

Tacheva-Grigorova, S.K., Santos, A.J.M., Boucrot, E. and Kirchhausen, T. (2013) Clathrin-Mediated Endocytosis Persists during Unperturbed Mitosis. Cell Rep. **4**, 659–668.

Takenawa, T. and Suetsugu, S. (2007) The WASP–WAVE protein network: connecting the membrane to the cytoskeleton. Nat. Rev. Mol. Cell Biol. **8**, 37–48.

Takenawa, T. and Miki, H. (2001) WASP and WAVE family proteins: key molecules for rapid rearrangement of cortical actin filaments and cell movement. J. Cell Sci. **114**, 1801–1809.

Tan, X., Heureaux, J. and Liu, A.P. (2015) Cell spreading area regulates clathrin-coated pit dynamics on micropatterned substrate. Integrative Biology **7**, 1033–1043.

Tank, D.W., Wu, E.S. and Webb, W.W. (1982) Enhanced molecular diffusibility in muscle membrane blebs: release of lateral constraints. J. Cell Biol. **92**, 207–212.

Taylor, M.J., Perrais, D. and Merrifield, C.J. (2011) A High Precision Survey of the Molecular Dynamics of Mammalian Clathrin-Mediated Endocytosis. PLOS Biol. **9**, e1000604.

Théry, M. and Bornens, M. (2006) Cell shape and cell division. Curr. Opin. Cell Biol. **18**, 648–657.

Thottacherry, J.J., Kosmalska, A.J., Kumar, A., Vishen, A.S., Elosegui-Artola, A., Pradhan, S., Sharma, S., Singh, P.P., Guadamillas, M.C., Chaudhary, N., Vishwakarma, R., Trepat, X., del Pozo, M.A., Parton, R.G., Rao, M., Pullarkat, P., Roca-Cusachs, P. and Mayor, S. (2018) Mechanochemical feedback control of

dynamin independent endocytosis modulates membrane tension in adherent cells. Nat. Commun. **9.**
Treusch, S., Hamamichi, S., Goodman, J.L., Matlack, K.E.S., Chung, C.Y., Baru, V., Shulman, J.M., Parrado, A., Bevis, B.J., Valastyan, J.S., Han, H., Lindhagen-Persson, M., Reiman, E.M., Evans, D.A., Bennett, D.A., Olofsson, A., DeJager, P.L., Tanzi, R.E., Caldwell, K.A., Caldwell, G.A. and Lindquist, S. (2011) Functional Links Between A Toxicity, Endocytic Trafficking, and Alzheimer's Disease Risk Factors in Yeast. Science **334**, 1241–1245.
Tsujita, K., Takenawa, T. and Itoh, T. (2015) Feedback regulation between plasma membrane tension and membrane-bending proteins organizes cell polarity during leading edge formation. Nat. Cell Biol. **17**, 749–758.
Tsygankova, O.M. and Keen, J.H. (2019) A unique role for clathrin light chain A in cell spreading and migration. J. Cell Sci. **132**, jcs224030.
Turlier, H. and Betz, T. (2019) Unveiling the Active Nature of Living-Membrane Fluctuations and Mechanics. Annu. Rev. Condensed Matter Phys. **10**, 213–232.
Unanue, E.R., Ungewickell, E. and Branton, D. (1981) The binding of clathrin triskelions to membranes from coated vesicles. Cell **26**, 439–446.
Ungewickell, E. and Branton, D. (1981) Assembly units of clathrin coats. Nature **289**, 420–422.
Vanden Broeck, D. and De Wolf, M.J.S. (2006) Selective blocking of clathrin-mediated endocytosis by RNA interference: epsin as target protein. BioTechniques **41**, 475–484.
Vassilopoulos, S., Gentil, C., Lainé, J., Buclez, P.-O., Franck, A., Ferry, A., Précigout, G., Roth, R., Heuser, J.E., Brodsky, F.M., Garcia, L., Bonne, G., Voit, T., Piétri-Rouxel, F. and Bitoun, M. (2014) Actin scaffolding by clathrin heavy chain is required for skeletal muscle sarcomere organization. J. Cell Biol. **205**, 377–393.
Vishwakarma, M., Di Russo, J., Probst, D., Schwarz, U.S., Das, T. and Spatz, J.P. (2018) Mechanical interactions among followers determine the emergence of leaders in migrating epithelial cell collectives. Nat. Commun. **9.**
Walani, N., Torres, J. and Agrawal, A. (2015) Endocytic proteins drive vesicle growth via instability in high membrane tension environment. Proc. Natl. Acad. Sci. **112**, E1423–E1432.
Walker, J.L., Fournier, A.K. and Assoian, R.K. (2005) Regulation of growth factor signaling and cell cycle progression by cell adhesion and adhesion-dependent changes in cellular tension. Cytokine & Growth Factor Reviews **16**, 395–405.
Wang, H., Rivenson, Y., Jin, Y., Wei, Z., Gao, R., Günaydın, H., Bentolila, L.A., Kural, C. and Ozcan, A. (2019) Deep learning enables cross-modality super-resolution in fluorescence microscopy. Nat. Methods **16**, 103–110.
Wang, X., Enomoto, A., Asai, N., Kato, T. and Takahashi, M. (2016) Collective invasion of cancer: Perspectives from pathology and development. Pathol. Int. **66**, 183–192.
Waugh, R.E. and Bauserman, R.G. (1995) Physical measurements of bilayer-skeletal separation forces. Ann. Biomed. Eng. **23**, 308–321.
Wessels, D., Reynolds, J., Johnson, O. and Soll, D. (2000) Clathrin plays a novel role in the regulation of cell polarity, pseudopod formation, uropod stability and motility in Dictyostelium. J. Cell Sci. **113**, 21–36.
Wettey, F.R. (2002) Controlled Elimination of Clathrin Heavy-Chain Expression in DT40 Lymphocytes. Science **297**, 1521–1525.
Wilbur, J.D., Hwang, P.K., Ybe, J.A., Lane, M., Sellers, B.D., Jacobson, M.P., Fletterick, R.J. and Brodsky, F.M. (2010) Conformation Switching of Clathrin Light Chain Regulates Clathrin Lattice Assembly. Dev. Cell **18**, 854–861.
Willy, N.M., Ferguson, J.P., Huber, S.D., Heidotting, S.P., Aygün, E., Wurm, S.A., Johnston-Halperin, E., Poirier, M.G. and Kural, C. (2017) Membrane mechanics govern spatiotemporal heterogeneity of endocytic clathrin coat dynamics. Mol. Biol. Cell **28**, 3480–3488.
Willly, N.M., Ferguson, J.P., Silahli, S., Cakez, C., Hasan, F., Chen, Y., Wu, M., Chang, H.C., Travesset, A., Li, S., Zandi, R., Li, D., Betzig, E., Cocucci, E., Kural C. (2019) Endocytic clathrin coats develop curvature at early stages of their formation. bioRxiv, 715219.
Wu, S., Majeed, S.R., Evans, T.M., Camus, M.D., Wong, N.M.L., Schollmeier, Y., Park, M., Muppidi, J.R., Reboldi, A., Parham, P., Cyster, J.G. and Brodsky, F.M. (2016) Clathrin light chains' role in selective endocytosis influences antibody isotype switching. Proc. Natl. Acad. Sci. **113**, 9816–9821.
Yarwood, R., Hellicar, J., Woodman, P.G. and Lowe, M. (2020) Membrane trafficking in health and disease. Dis. Models Mech. **13**, dmm043448.
Ybe, J.A. (1998) Clathrin self-assembly is regulated by three light-chain residues controlling the formation of critical salt bridges. EMBO J. **17**, 1297–1303.
Zuidema, A., Wang, W., Kreft, M., te Molder, L., Hoekman, L., Bleijerveld, O.B., Nahidiazar, L., Janssen, H. and Sonnenberg, A. (2018) Mechanisms of integrin $\alpha V\beta 5$ clustering in flat clathrin lattices. J. Cell Sci. **131**, jcs221317.

Received: 19 August 2020; Revised: 8 March 2021; Accepted: 19 March 2021; Published online: 31 March 2021

